

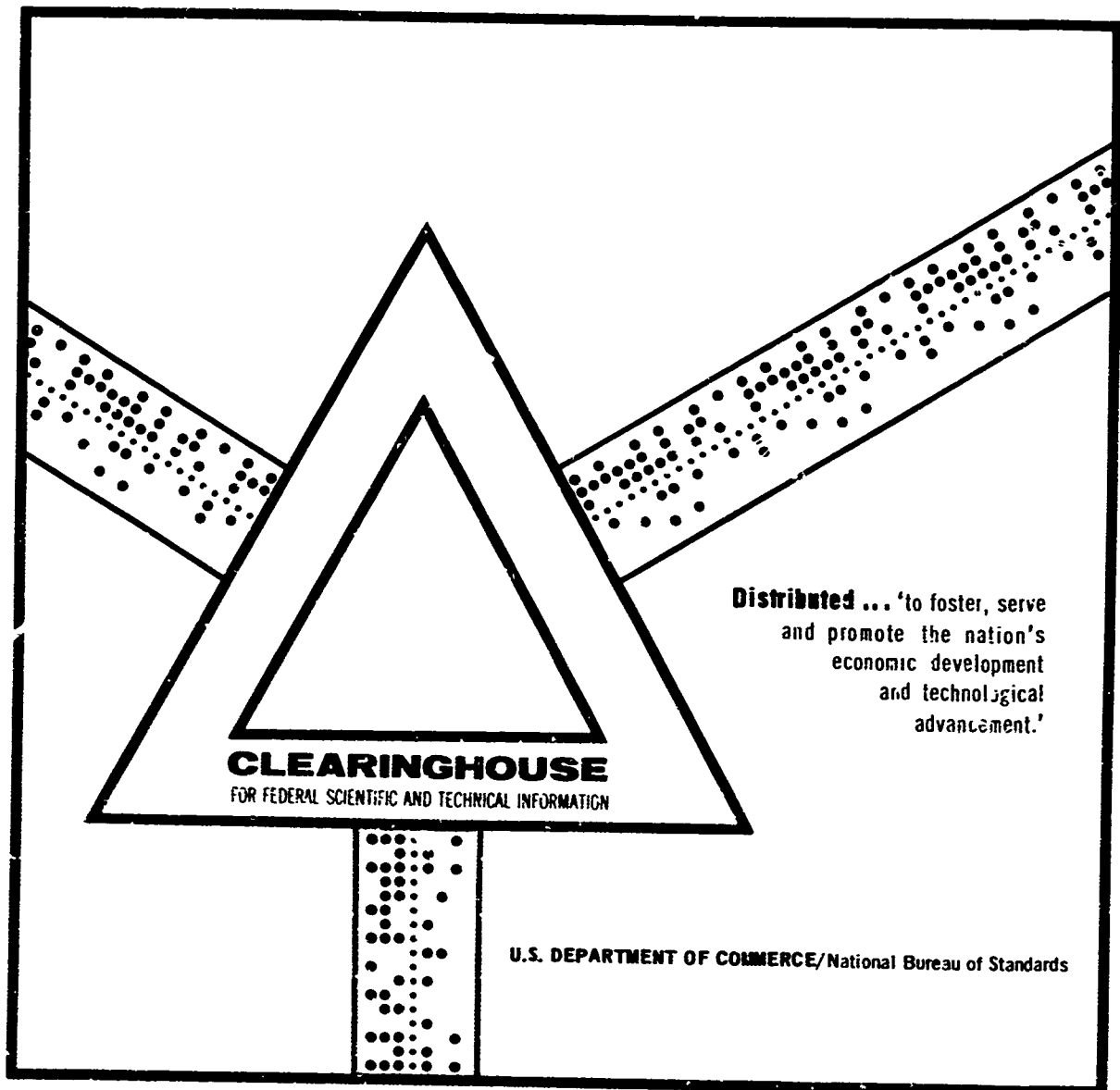
AD 696 100

ROCKET INSTRUMENTATION FOR PCA MEASUREMENTS-  
BLACK BRANT 17.750 AND 17.751

David A. Burt

Utah University  
Salt Lake City, Utah

June 1969



This document has been approved for public release and sale.

AFCRL69-0282

UU69-2

AD696100

UURL

ROCKET INSTRUMENTATION  
FOR PCA MEASUREMENTS-  
BLACK BRANT 17.750 AND 17.751

by

David A. Burt

Contract No. F19628-67-C-0275

Project No. 5710

SCIENTIFIC REPORT NO. 3

June 1969

Contract Monitor: James C. Ulwick  
Ionospheric Physics Laboratory

Distribution of this document is unlimited. It may be released to the  
Clearinghouse, Department of Commerce, for sale to the general public.

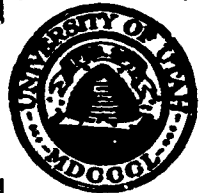
This research was supported  
by the Defense Atomic Support Agency.

Prepared for

Air Force Cambridge Research Laboratories  
Office of Aerospace Research  
United States Air Force  
Bedford, Massachusetts 01730

NOV 12 1969

UPPER AIR RESEARCH LABORATORY  
University of Utah Salt Lake City, Utah / 84112



Produced by the  
CLEARINGHOUSE  
for Federal Scientific & Technical  
Information Springfield Va. 22151

8i

Qualified requestors may obtain additional copies from the Defense Documentation Center. All others should apply to the Clearinghouse for Federal Scientific and Technical Information.

ACCESSION

CFSTI  
DDC  
d ANOMAS P  
JULY 1982

BY  
DISTRICT OF COLUMBIA

8182

--	--	--

AFRCL-69-0282

UU-69-2

ROCKET INSTRUMENTATION FOR PCA MEASUREMENTS-  
BLACK BRANT 17.750 AND 17.751

by

David A. Burt

Upper Air Research Laboratory  
University of Utah  
Salt Lake City, Utah 84112

Contract No. F19628-67-C-0275  
Project No. 5710

Scientific Report No. 3

June 1969

Distribution of this document is unlimited. It may be released to the Clearinghouse, Department of Commerce, for sale to the general public.

Contract Monitor: James C. Ulwick  
Ionospheric Physics Laboratory

This research was supported by the  
Defense Atomic Support Agency

Prepared For

Air Force Cambridge Research Laboratories  
Office of Aerospace Research  
United States Air Force  
Bedford, Massachusetts 01730

Submitted by

*Hayden Baker*  
Obed C. Haycock, Director

## ABSTRACT

This report discusses instruments contained in the payloads of Black Brants 17.750 and 17.751. These instruments were designed to measure characteristics of the D-region associated with polar cap absorption (PCA) events. The measurements included proton fluxes, x-ray emissions, total particle energy deposition, Lyman- $\alpha$  radiation, electron and ion densities and temperatures, and photometric emissions in the ionosphere.

LIST OF CONTRIBUTORS - SCIENTISTS AND ENGINEERS

O.C. Haycock	Director
K.D. Baker	Assistant Director
D.A. Burt	Project Engineer
L.C. Howlett	Research Engineer
E.F. Pound	Senior Research Engineer
K.G. Seljaas	Research Engineer

RELATED CONTRACTS AND PUBLICATIONS

AF 19(628)-5044

AF 19(628)-4995

Burt, D.A. Rocket instrumentation for auroral measurements - Black Brant AC 17.604, *Scientific Report No. 7*, Contract No. AF 19(628)-4995, AFCRL 67-0295, UU-67-1, March 1967.

Phillips, K.E., Determination of the aspect for instruments in a rocket payload, *Scientific Report No. 2*, Contract No. F19628-67-C-0275, AFCRL 69- , UU-69-1, April 1969.

Seljaas, K.G., Langmuir probes for determining ionospheric particle densities and temperatures, *Scientific Report No. 1*, Contract No. F19628-67-C-0275, AFCRL-68-0306, UU-68-2, June 1968.

Ulwick, J.C., W. Pfister, and K.D. Baker, Rocket measurements of bremsstrahlung x rays and related parameters during auroral absorption events, in *Space Research VIII*, edited by A.P. Mitra, L.G. Jacchia, and W.S. Newman, p. 171, North Holland Publishing Co., Amsterdam, 1968.

## TABLE OF CONTENTS

	<u>Page</u>
Abstract . . . . .	i
List of Contributors . . . . .	ii
Table of Contents . . . . .	iii
List of Illustrations . . . . .	iv
List of Tables . . . . .	vi
Preface . . . . .	vii
 INTRODUCTION . . . . .	 1
 INSTRUMENTATION . . . . .	 8
Standing Wave Impedance Probe (SWIP) . . . . .	8
X-ray Counter . . . . .	15
Energy Deposition Scintillator . . . . .	15
Lyman- $\alpha$ Detector . . . . .	20
Langmuir Probe . . . . .	30
Filter Wheel Photometer . . . . .	30
Telemetry System . . . . .	45
Trajectory and Aspect Systems . . . . .	45
 RESULTS AND CONCLUSION . . . . .	 51
 APPENDIX A - Calibrations and General Information . . . . .	 55
 APPENDIX B - Photometer Filter Characteristics and Phototube Response . . . . .	 66

LIST OF ILLUSTRATIONS

<u>Figure</u>		<u>Page</u>
1	Day night variation of a PCA event . . . . .	2
2	Photograph of the payload of Black Brant 17.751 . .	6
3	Drawing of payloads showing experiment positions . .	7
4	Calibration of 17.751 antenna potential monitor . .	10
5	Calibration of 17.750 antenna potential monitor . .	11
6	Schematic drawing of antenna potential monitors . .	12
7	Block diagram of the Z6 probe . . . . .	14
8	Fields of view for proportional x-ray counter . . .	16
9	Energy resolution of the 17.750 x-ray counter . . .	17
10	Energy resolution of the 17.751 x-ray counter . . .	18
11	X-ray counter tube efficiency . . . . .	19
12	Energy deposition scintillator - schematic diagram .	21
13	Calibration of 17.750 energy deposition scintillator	22
14	Calibration of 17.751 energy deposition scintillator	23
15	Photograph of Lyman- $\alpha$ detector . . . . .	24
16	Schematic diagram of Lyman- $\alpha$ detector . . . . .	26
17	Lyman- $\alpha$ high voltage monitor calibration . . . . .	27
18	Lyman- $\alpha$ detector (17.750) - system calibration . . .	28
19	Lyman- $\alpha$ detector (17.751) - system calibration . . .	29
20	Photograph of the 17.751 Langmuir probe . . . . .	31
21	Sweep wave form of the 17.751 Langmuir probe . . . .	32
22	Ion mode calibration - 17.751 Langmuir probe . . . .	33
23	Electron mode calibration - 17.751 Langmuir probe .	34
24	Sweep wave form of the 17.750 Langmuir probe . . . .	35
25	Ion mode calibration - 17.750 Langmuir probe . . . .	36
26	Electron mode calibration - 17.750 Langmuir probe .	37
27	Photograph of the filter wheel photometer . . . . .	38
28a	Photometer calibrations (17.750) - filters 1 and 2 .	39
28b	Photometer calibrations (17.750) - filters 3 and 4 .	40
28c	Photometer calibrations (17.750) - filters 5 and 6 .	41
29a	Photometer calibrations (17.751) - filters 1 and 2 .	42
29b	Photometer calibrations (17.751) - filters 3 and 4 .	43

LIST OF ILLUSTRATIONS (cont.)

<u>Figure</u>		<u>Page</u>
29c	Photometer calibrations (17.751) - filters 5 and 6 .	44
30	Photometer high voltage monitor calibration . . . . .	46
31	Photometer temperature monitor calibration . . . . .	47
32	Trajectory of Black Brant 17.750 . . . . .	52
33	Picture of recovered Black Brant 17.751 . . . . .	53
A-1	Dimensions and orientation of SWIP antenna . . . . .	63
A-2	Z $\theta$ probe calibration curves at 3 MHz . . . . .	64
A-3	Z $\theta$ probe calibration curves at 7.2 MHz . . . . .	65
B-1a	Photometer transmission curves (17.750) - filters 1, 2, and 3 . . . . .	66
B-1b	Photometer transmission curves (17.750) - filters 4, 5, and 6 . . . . .	67
B-2a	Photometer transmission curves (17.751) - filters 1, 2, and 3 . . . . .	68
B-2b	Photometer transmission curves (17.751) - filters 4, 5, and 6 . . . . .	69
B-3	Photometer composite spectral response (17.750) . .	70
B-4	Photoemissive response for S11 photomultiplier cathodes . . . . .	71

LIST OF TABLES

<u>Table</u>		<u>Page</u>
1	Payload of Black Brant 17.750 . . . . .	3
2	Payload of Black Brant 17.751 . . . . .	4
3	Commutator Assignment for SWIP . . . . .	9
4	Frequency Indicator Voltage Outputs (SWIP) . . . . .	9
5	Commutator Assignment for Z $\theta$ Probe . . . . .	13
6	Energy Deposition Scintillator Characteristics . . . . .	16
7	Lyman- $\alpha$ Detector Characteristics . . . . .	27
8	Specifications for Photometer on 17.750 . . . . .	35
9	Specifications for Photometer on 17.751 . . . . .	45
10	Telemetry Assignments - Link 1 . . . . .	48
11	Telemetry Assignments - Link 2 . . . . .	49
12	Commutator Data Assignments . . . . .	50

## PREFACE

At the University of Utah a number of individuals had specific responsibilities for different phases of the project reported herein:

Administration	Obed C. Haycock
Project scientist	Kay D. Baker
Project engineer	David A. Burt
Langmuir probe	Karl G. Seljaas
X-ray counter	L. Carl Howlett
Energy deposition scintillator	L. Carl Howlett
Z $\theta$ probe	David A. Burt
Lyman- $\alpha$ detector	David A. Burt
Filter wheel photometer	Doran J. Baker*
Mechanical fabrication	Karl Dunn
Editing	Russell J. Richards
Illustrations	Robert M. Fowler
Field operations	David A. Burt, Kay D. Baker, and Fred Riebeck

\* The filter wheel photometer was supplied by Electrodynamic Laboratory, Utah State University, Logan, Utah.

## INTRODUCTION

This report details the scientific instrumentation in two Black Brant rockets (17.750 and 17.751). The rockets considered in this report are only two of a large series of rockets which are assigned to measure certain disturbed characteristics of the D-region during special disturbed conditions called polar cap absorption (PCA) events. The term polar cap absorption refers to the extreme absorption of certain radio frequencies, especially in the HF range, as radio waves pass through the D-region of the ionosphere. Such events occur rarely since they result only from a few large solar flares that emit energetic protons which intensely ionize the mesosphere. These events disrupt communications for several days at higher latitudes (above approximately  $65^{\circ}$  geomagnetic latitude).

Riometers indicate that a PCA event normally begins a few hours after these solar flares occur and first interrupts communications at latitudes from  $65^{\circ}$  to  $90^{\circ}$ , but it soon encompasses the whole polar region. The absorption quickly reaches a maximum and then decays over a period of days. Figure 1 shows that the absorption decreases noticeably at night and causes a definite modulation of the otherwise relatively smooth absorption profile. The "quiet day" curve, the upper curve in the figure, is the average of a year's data and is thus independent of any one day. The lower curve represents the actual riometer readings for the time periods shown. Increased absorption is exhibited by the decreases in the receiver current (milliamps).

The majority of the rockets in the large series, mentioned above, are provisionally scheduled to be flown within the same twenty-four hour period in the latter part of 1969 to measure the day-night variation of a PCA event. The instrumentation aboard all the rockets in this series will measure parameters such as proton fluxes, total particle energy deposition, electron and ion densities and temperatures, and photometric emissions in the ionosphere.

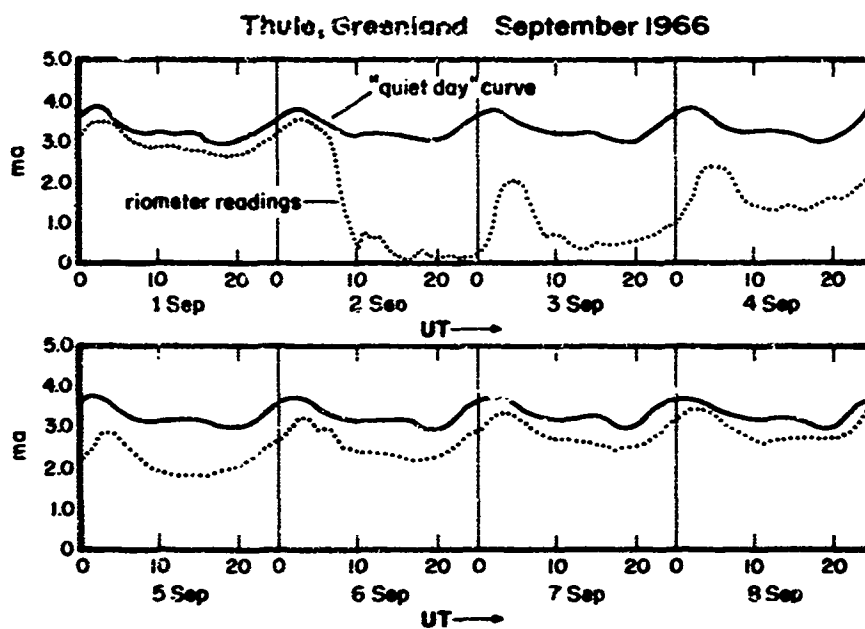


Fig. 1. Day-night variation of a PCA event. The solid line represents the average of a year's data. The dotted line shows the increased absorption of the radio waves due to the PCA phenomenon which occurred between 1 and 8 September 1966 above Thule, Greenland.

Measurements of the whole PCA rocket series, with supporting tests by aircraft, satellite, and ground-based instruments, will provide a comprehensive study of the PCA phenomenon.

To obtain prior verification of the multiple instrumentation in the Black Brant payload design, Black Brants 17.750 and 17.751 were scheduled to be flown in conjunction with each other within a twenty-four hour period: one to be flown in the daytime and the other to be flown at night. Tables 1 and 2 list the instruments flown on these rockets. Black Brant 17.750 was launched from the Churchill Research Range at 10:14:51.46 CST on 6 December 1967. Black Brant 17.751 was launched from the Churchill Research Range at 15:51:02.43 CST on 10 June 1968. The separation of flight dates was due primarily to a scarcity of PCA events. After integration of these two payloads, 17.750 was fired into an auroral absorption event, rather than waiting an indefinite length of time for veri-

fication of the payload in a PCA event. Black Brant 17.751 was launched into a PCA event but due to abnormal flight dynamics, the payload separated and failed to provide any PCA measurements.

TABLE 1. Payload of Black Brant 17.750

Instrument	Agency	Measurements
Standing wave impedance probe (SN-98)	University of Utah	Electron density
X-ray counter (Model 2, SN-3)	University of Utah	X rays, 1-10 kev
Energy deposition scintillator (Model 3, SN-1)	University of Utah	Energy deposition Electrons > 9 kev Protons > 60 kev
Lyman- $\alpha$ detector (Model La-67, SN-2)	University of Utah	Lyman- $\alpha$ radiation, 1216 A
Langmuir probe (Model LP-67-C, SN-1)	University of Utah	Electron density and temperature, positive ion density
Filter wheel photometer (Model WT-1B, SN-22-FW1)	Utah State University	Light emissions; N <sub>2</sub> (3914A), O (5577A) <sup>2</sup> , NO <sub>2</sub> continuum (5775A), H $\beta$ <sup>2</sup> (4861A), background (4020A, 3800A)
Gerdien condensers (3)	Adcole Corporation	Conductivity, ion and electron density
Retarding potential analyzer	Adcole Corporation	Positive ion density
Propagation experiment	Pennsylvania State	Electron density
DC probe (blunt)	Pennsylvania State	Positive and negative charge density
Conductivity probe	Pennsylvania State	Electron density
Proton detector (A)	Panametrics, Inc.	Protons, 1.65 to 3.2 mev Alphas, 4.2 to 19.6 mev (Horizontal look direction)
Proton detector (B)	Panametrics, Inc.	Protons, 3.2 to 100 mev Alphas, 5.1 to 190 mev (Horizontal look direction)

TABLE 2. Payload of Black Brant 17.751

Instrument	Agency	Measurements
Impedance probe (Standing wave and Z <sub>0</sub> probe 67-1)	University of Utah	Electron density
X-ray counter (Model 4, SN-1)	University of Utah	X rays, 1-10 kev
Energy deposition scintillator (Model 4, SN-1)	University of Utah	Energy deposition Electrons E > 9 kev Protons E > 60 kev
Lyman- $\alpha$ detector (Model La-67A, SN-1)	University of Utah	Lyman- $\alpha$ radiation, 1216 A
Langmuir probe (Model B)	University of Utah	Electron density and temperature, positive ion density
Filter wheel photometer (Model WT-1B, SN-23-FW1)	Utah State University	Light emissions, N <sub>2</sub> (3914A), O (5577A) <sup>2</sup> , NO <sub>2</sub> continuum (5775A), H $\beta$ <sup>2</sup> (4861A), background (4020A, 3800A)
Gerdien condensers (3)	Adcole Corporation	Conductivity, ion and electron density
Retarding potential analyzer	Adcole Corporation	Positive ion density
Propagation experiment	Pennsylvania State	Electron density
DC probe (blunt)	Pennsylvania State	Positive and negative conductivity
Conductivity probe	Pennsylvania State	Electron density
Proton detector (A)	Panametrics, Inc.	Protons, 1.65 to 3.2 mev Alphas, 4.2 to 19.6 mev (15° above horizontal)
Proton detector (B)	Panametrics, Inc.	Protons, 3.2 to 100 mev Alphas, 5.1 to 190 mev (15° above horizontal)

A number of agencies were involved in the experiments on these rockets. The only instruments which will be covered in detail are those developed by the University of Utah and Utah State University for Air Force Cambridge Research Laboratories.

Figures 2 and 3 display the payload configuration of Black Brant 17.750. Figure 2 is a photograph of the payload. A nose and side view of the payload is diagrammatically represented in Figure 3.



Fig. 2. Photograph of the payload of Black Brant 17.751.

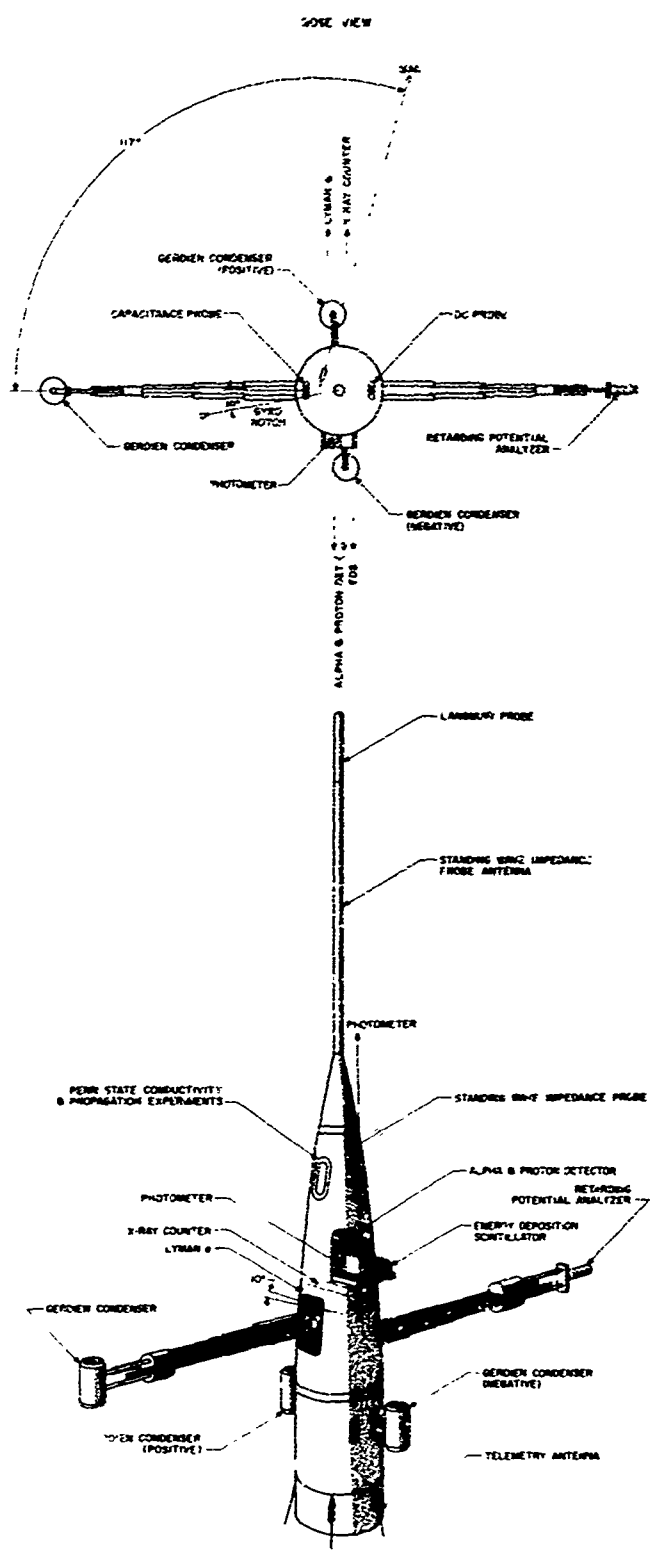


Fig. 3. Drawing of the 17.750 and 17.751 payloads showing the relative positions of experiments.

## INSTRUMENTATION

### Standing Wave Impedance Probe (SWIP)

The standing wave impedance probe measures electron density by determining the impedance change of a 2-meter long nose-spike antenna as the rocket proceeds through an ionized media. The impedance is measured at 3 and 7.2 MHz by applying these frequencies through a segmented lumped constant delay line. A commutator samples the voltage on each segment of the delay line to determine the standing wave ratio and the minimum and maximum voltage positions. This information when telemetered to ground is sufficient to determine the antenna impedance.

The basic design of the SWIP experiment tested on Black Brant 17.604 [Burt, 1967], with a Langmuir probe at the end of its nose-spike antenna, was also used in Black Brants 17.750 and 17.751. Previous flights indicated the desirability of some changes that were incorporated in these last two rockets to improve the accuracy of the results. Test flights have indicated that the application of an RF voltage to a large surface antenna changes the vehicle potential (a rectification process due to the nonlinearity of the ionosphere) [Seljaas and Burt, 1967]. The amount of this change was found to be a function of the frequency applied to the antenna: the lower the frequency, the higher the voltage swing. Sensitive instruments on these two rockets required a relatively stable vehicle potential which made a minimum swing of potential desirable. To stabilize vehicle potential for longer periods of time, the former sweeping sequence of 17.604 was changed so that the higher frequency was applied for extended numbers of sweeps, and to minimize the swing of vehicle potential the 2 MHz frequency in the sequence was changed to 3 MHz. The following frequency switching sequence was used: seven commutator rotations at 7.2 MHz, one rotation at 3 MHz, seven rotations at 7.2 MHz, one rotation with no RF applied to the antenna.

In order to study the changes in vehicle potential due to changes in the applied RF voltages (the rectification process above), a high impedance amplifier was installed to monitor the dc voltage between the antenna and the rocket body. While the output of this amplifier was applied to a continuous channel on 17.750, on 17.751 this output was commutated with the Z $\theta$  probe output. The calibration curves of the antenna potential monitors on the two rockets are presented in Figures 4 and 5. A schematic configuration of the antenna potential monitor is represented in Figure 6.

The format for the SWIP commutators is a 5 x 30 RZ IRIG. The assignment for the standing wave impedance probes is shown in Table 3.

TABLE 3. Commutator assignment for SWIP instruments on 17.750 and 17.751

Segment Number	Assignment
1	sync pulse
2	+ 5 volt reference voltage
3	+ 1 volt reference voltage
4	floating point
5-28	standing wave voltage
29	frequency indicator

The frequency indicator for the SWIP experiments output is given in Table 4.

TABLE 4. Frequency indicator voltage outputs for 17.750 and 17.751

Frequency Indicator	Frequency
3.8 volts	7.2 MHz
2.0 volts	3.0 MHz

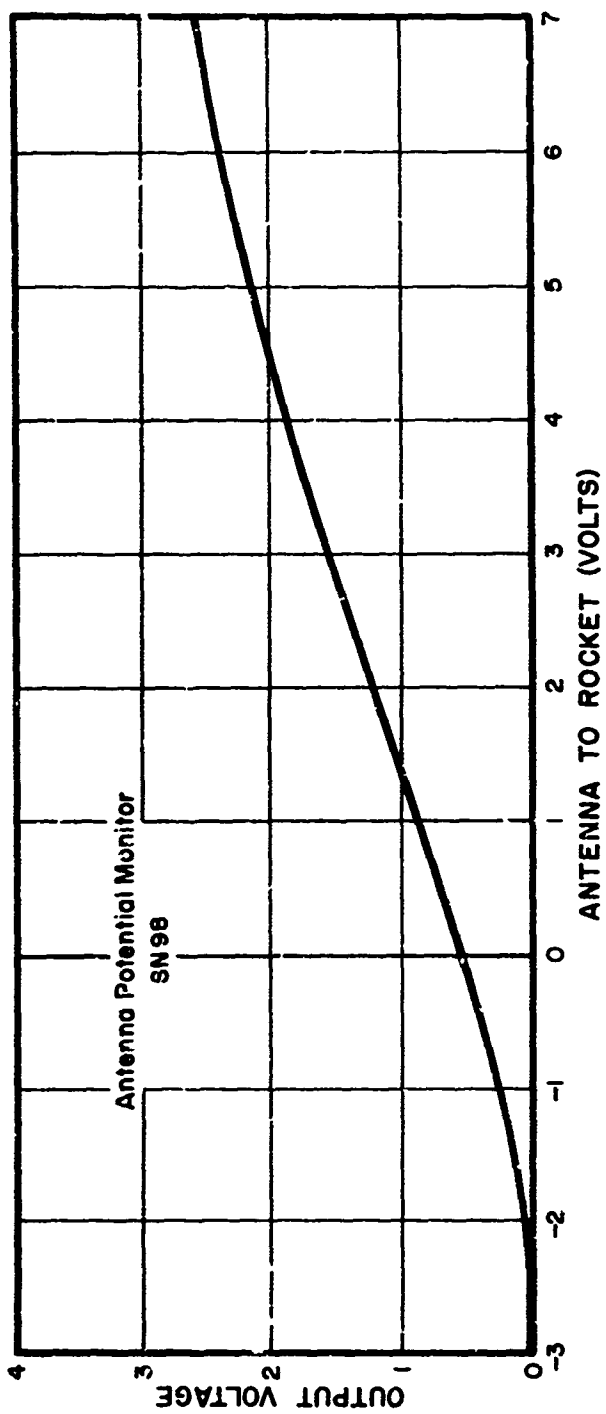


Fig. 4. Calibration curve of the antenna potential monitor on the 17.750 SWIP (SN-98).

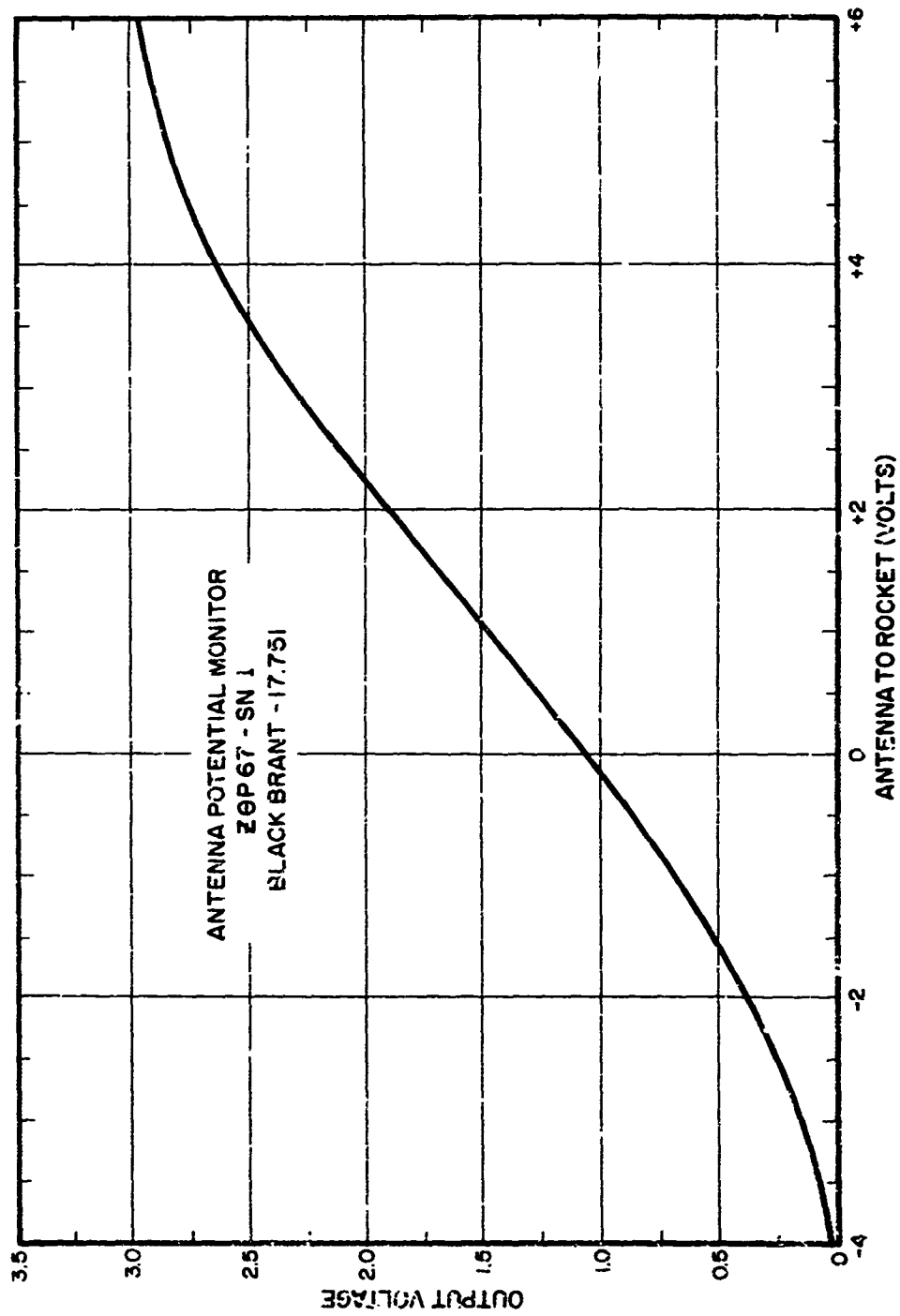


Fig. 5. Calibration curve of the antenna potential monitor on the Z6 probe (Model 67, SN-1).

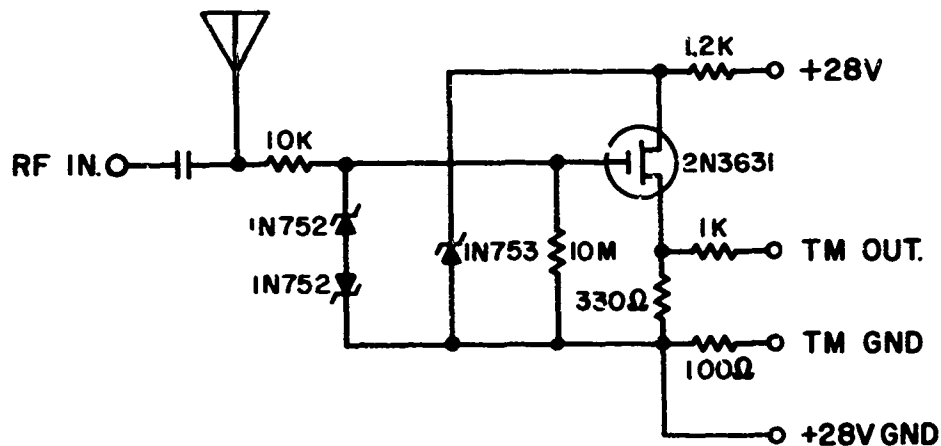


Fig. 6. Schematic drawing of the antenna potential monitor flown on both Black Brants.

Complete calibrations of the standing wave impedance probe and the antenna measurements are given in the Appendix A. Further details and complete schematic designs of the standing wave impedance probe have been presented in earlier reports [Ulwick, *et al.*, 1967; Seljaas and Burt, 1967; Burt, 1967].

#### Z $\theta$ Probe (Black Brant 17.751)

The one minor difference between the two rockets was the introduction of a new method of measuring the antenna impedance. In addition to the standard SWIP instrument, which was utilized in tests aboard both rockets, the new method (designated the Z $\theta$  probe) was used aboard 17.751. The Z $\theta$  probe directly measures the magnitudes of the antenna current and voltage and the phase angle between the antenna current and voltage; thus the complete antenna impedance can be easily calculated and related to electron density. The Z $\theta$  probe

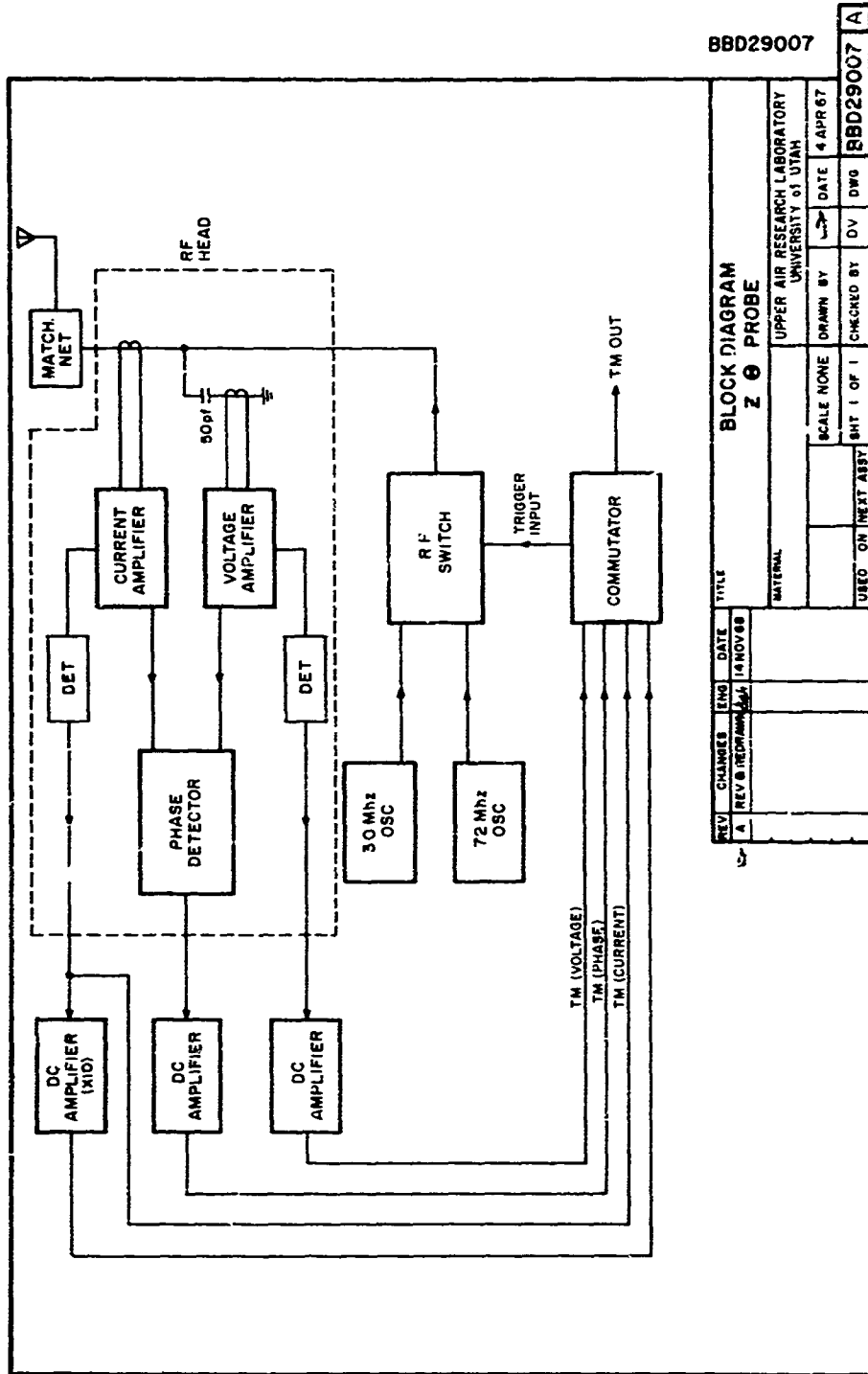
has numerous advantages over the standing wave impedance probe: a narrower telemetry bandwidth can be used; more direct data reduction methods can be utilized; and inherent inaccuracies in the determination of line parameters can be eliminated.

The Z $\theta$  probe, like the standing wave impedance probe, is used to detect the antenna impedance. Figure 7 presents a block diagram of the Z $\theta$  probe system. The impedance is determined by measuring the magnitude of the antenna current and voltage using two high gain amplifiers which are transformer-coupled to the antenna. One amplifier is coupled in series with the antenna to measure the current while the second amplifier is coupled in parallel to measure the voltage. The outputs of these amplifiers are detected resulting in dc voltages which are proportional to the antenna current and voltage. The antenna current monitor is also magnified by a factor of 10 by a second amplifier to give greater sensitivity at low current values. The output from each amplifier is fed into a clipper amplifier which squares the waveform so that the phase relationship between the waveforms of the two amplifiers can be detected more readily. The outputs from the clipper amplifiers are then fed into a detector which measures the phase relationship between the two waveforms and results in a dc voltage output which is proportional to the phase between the antenna current and voltage.

The outputs of the Z $\theta$  probe were commutated; the commutator assignment for the Z $\theta$  probe is presented in Table 5.

TABLE 5. Commutator assignment for the Z $\theta$  probe flown on 17.751

Segment Number	Assignment
1	+ 5 v reference
2	0 v reference
3	antenna current
4	phase of impedance
5	antenna voltage
6	antenna current x 10
7	antenna potential monitor



88D29007

REV		CHANGES	ENG	DATE	TITLE		
1	A	REV B (REPROGRAM)	14	NOV 68	BLOCK DIAGRAM Z 0 PROBE		
MATERIAL					UPPER AIR RESEARCH LABORATORY UNIVERSITY OF UTAH		
SCALE NONE					DRAWN BY	DATE	4 APR 67
USED ON NEXT ASST					SHT 1 OF 1	CHECKED BY	DWG 88D29007 A

Fig. 7. Block diagram of the Z0 probe (17.751).

Appendix A contains the complete calibration curves of the Z0 probe.

#### X-ray Counter

An x-ray counter was included on each rocket to measure the input flux and energy spectrum from soft x rays. The unit uses a proportional counter tube and associated circuitry to broaden the output pulses for telemetry transmission. This information can be fed directly to a pulse height analyzer to separate the different energies. Comprehensive pictures and schematic drawings of this instrument are given in previous reports [Burt, 1967; Howlett, 1966].

Each x-ray counter was mounted to view through a door in the side of the rocket skin (Figure 3) and was tilted  $10^\circ$  above the horizontal in order to include the sun in the field of view as the rocket rolled. The field of view of each instrument, as shown in Figure 8, was  $21.5^\circ$  vertical and  $8^\circ$  horizontal for the half angle at the half count points. The field of view, with an aperture area of 0.23 cm, gives a geometric factor of  $4.5 \times 10^{-2} \text{ cm}^2 \text{ ster}$ . Calibrations to determine the energy conversion factor and resolution of the instruments were performed with an Fe-55 source (5.9 kev or 2.1 A x rays). The results of calibration for 17.750 are shown in Figure 9, and the results for 17.751 are shown in Figure 10. The conversion factors are 3.18 kev/volt for 17.750 with 34% resolution and 2.46 kev/volt for 17.751 with 26.1% resolution. The counter tube efficiency is presented in Figure 11.

#### Energy Deposition Scintillator

The energy deposition scintillator is designed to measure the total energy being deposited by particles in a given region of the atmosphere. This is accomplished by sensing the light output of a scintillation crystal with a photomultiplier tube and by amplifying the output with a logarithmic amplifier for telemetry transmission.

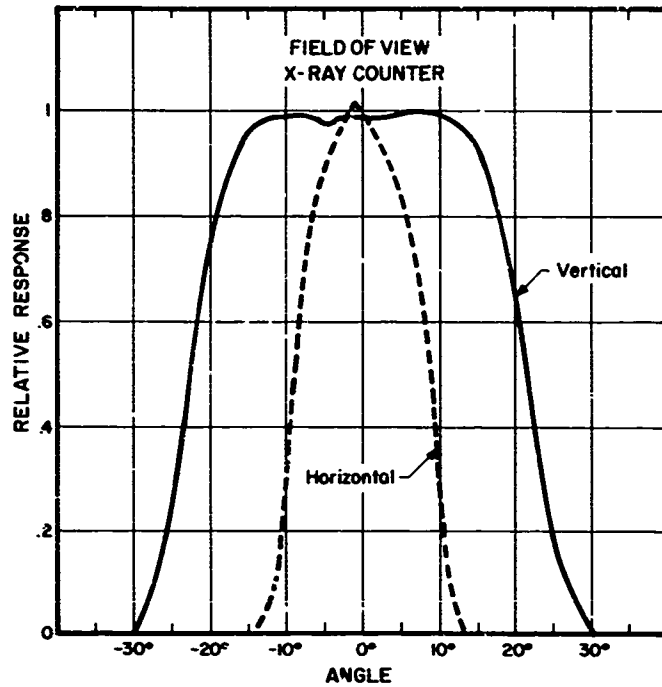


Fig. 8. Fields of view for the proportional x-ray counters.

The logarithmic amplifier consists of an operational amplifier with temperature-controlled diode feedback network to obtain the desired characteristics. The scintillator utilizes a pilot B plastic crystal. This crystal is sealed from light by vacuum depositing a thin layer of aluminum over the surface. The characteristics of the two instruments are given in Table 6.

TABLE 6. Energy Deposition Scintillator Characteristics

	17.750 Model 3 SN1	17.751 Model 4 SN1
Aluminum deposition thickness	5600A	6200A
Lower cutoff energy	8 kev	10 kev
Output with luminous intensity of 12,000 foot-candles (sun = 8,800 foot-candles)	0.7 volts	1.20 volts
Aperture area	0.203 cm <sup>2</sup>	0.203 cm <sup>2</sup>
Half angle field of view	12°	12°
Geometric factor	2.8 x 10 <sup>-2</sup> cm <sup>2</sup> ster	2.8 x 10 <sup>-2</sup> cm <sup>2</sup> ster

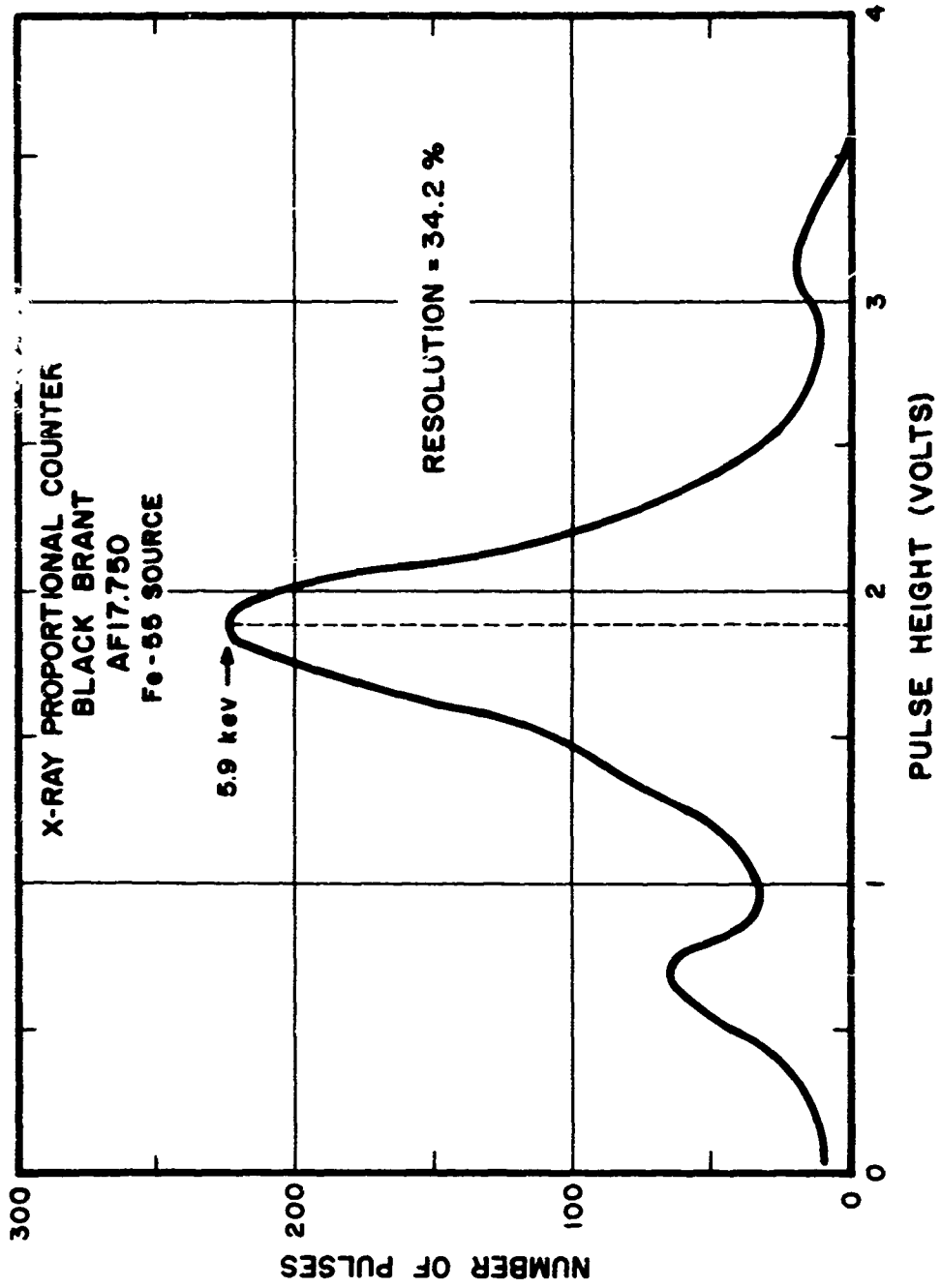


Fig. 9. Energy resolution of the 17.750 proportional x-ray counter (Model 2, SN-3).

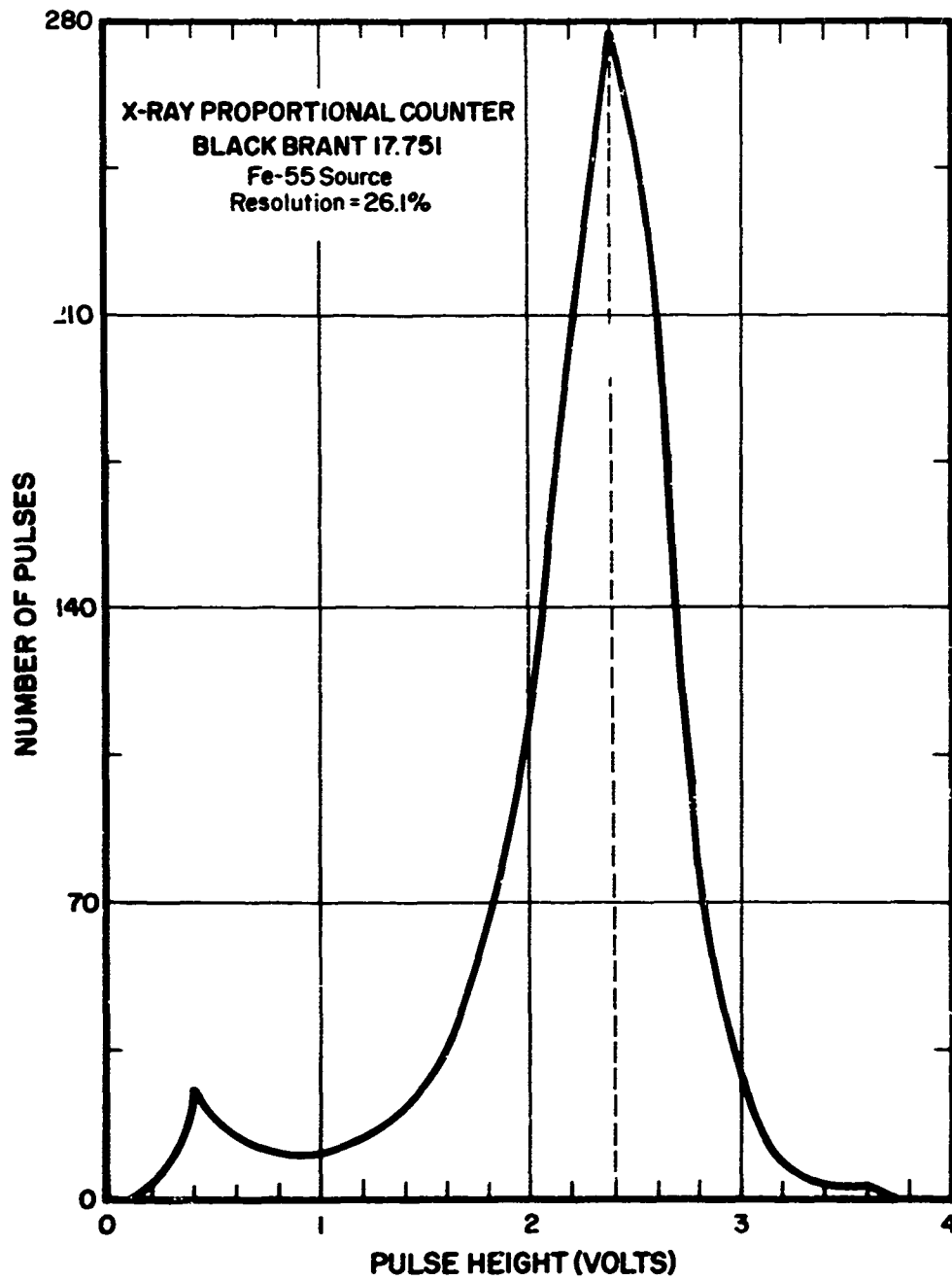


Fig. 10. Energy resolution of the 17.751 proportional x-ray counter (Model 4, SN-1).

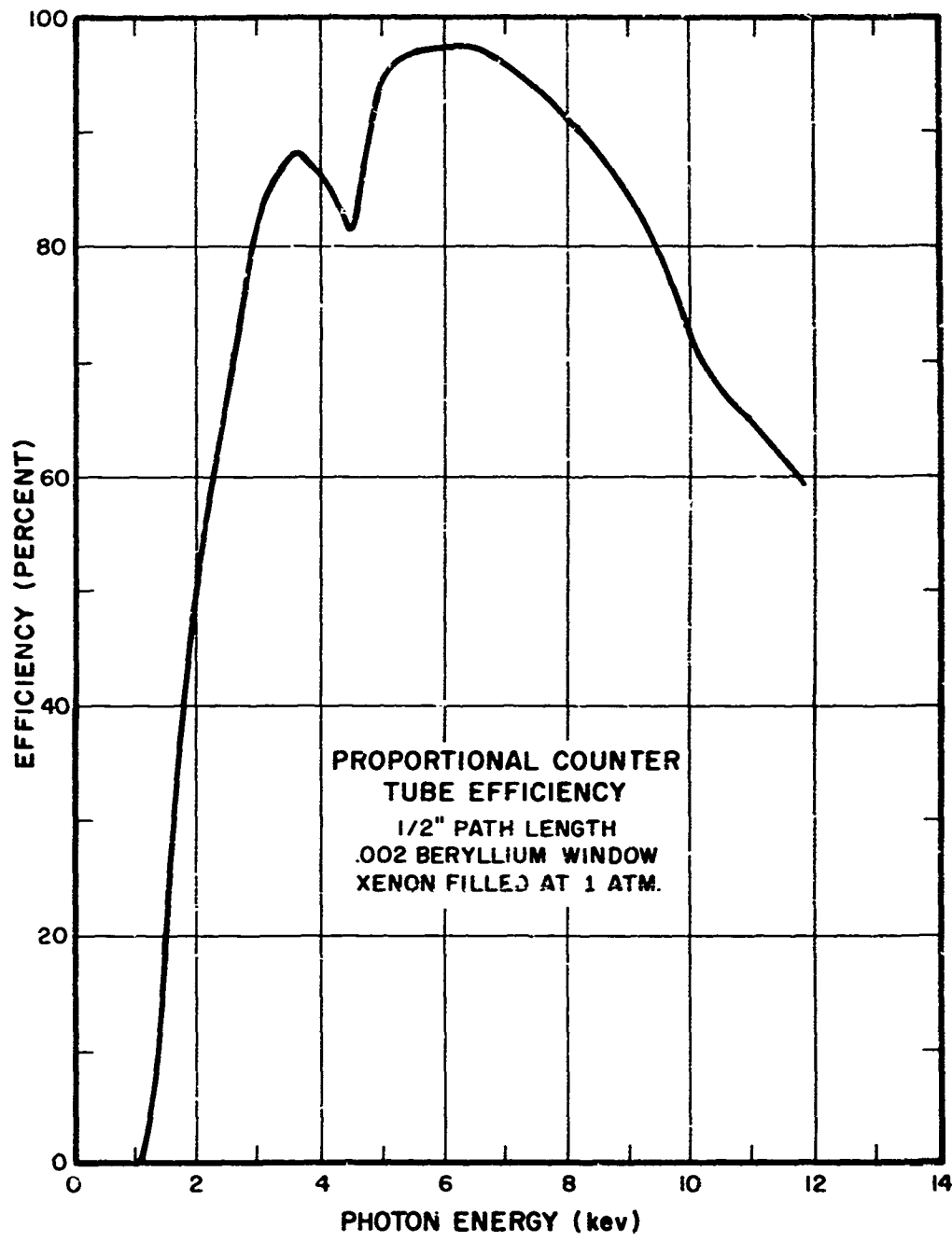


Fig. 11. X-ray counter efficiency as a function of photon energy.

The instruments flown on the two rockets were basically the same except that the unit on 17.751 utilized an improved voltage regulator. A complete schematic diagram of the energy deposition scintillator used on 17.751 is given in Figure 12.

Calibration of these instruments was accomplished by determining the voltage current characteristics of the logarithmic amplifier of each and then determining a point on this curve for a known energy source. The source used was a nickel 63 with a calibrated total output of  $\frac{0.87 \times 10^{11} \text{ ev/s}}{2\pi \text{ ster}}$ . The maximum particle energy was 65 kev with an average energy of 18 kev. The calibration curve obtained for 17.750 (Model 3, SN-1) is shown in Figure 13. Figure 14 shows the calibration curve derived for 17.751 (Model 4, SN-1).

#### Lyman- $\alpha$ Detector

In order to determine the degree of ionization due to Lyman- $\alpha$  radiation, a detector (pictorially illustrated in Figure 15) was used to measure the intensity of Lyman  $\alpha$  (1216 A). The detector was a nitric oxide (NO) photoionization chamber with a lithium fluoride window (Melpar No. CGGL 1350). The solar Lyman- $\alpha$  intensity is about 5 ergs/cm<sup>2</sup> [Hinteregger, 1965]. The instrument was therefore set for a maximum energy about an order of magnitude higher or 50 ergs/cm<sup>2</sup>.

The ionization chamber current due to a source entirely in the field of view (such as the sun) will be

$$i = \frac{IAN}{E}$$

where

- i = current in amperes
- I = radiant energy in watts/cm<sup>2</sup>
- A = detector area in cm<sup>2</sup>
- $\eta$  = chamber quantum efficiency
- E = photon energy in electron volts

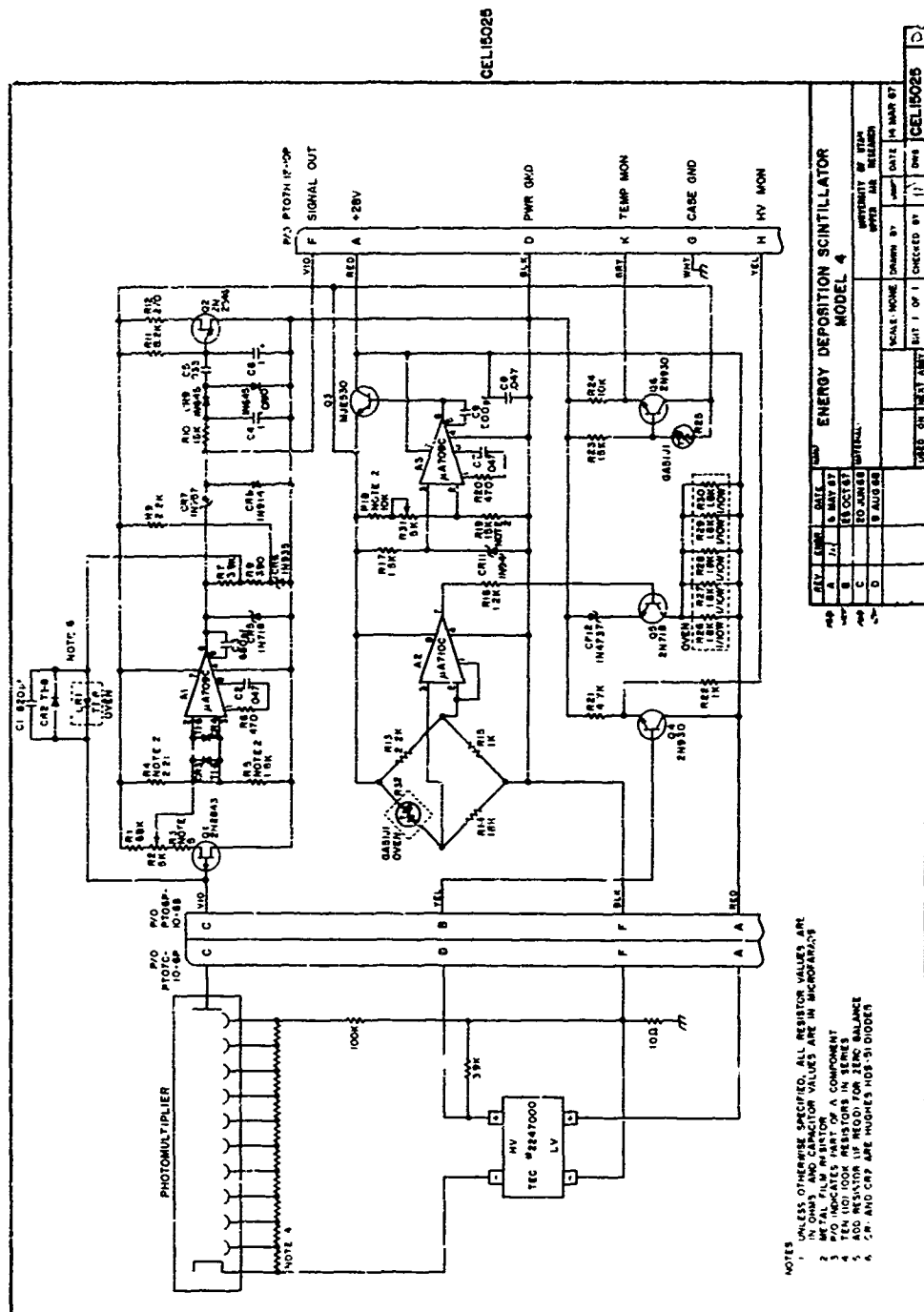


Fig. 12. Schematic diagram of the 17.751 energy deposition scintillator (Model 4, SN-1). The voltage regulator on this unit was an improved modification of the 17.750 EDS (Model 3, SN-1).

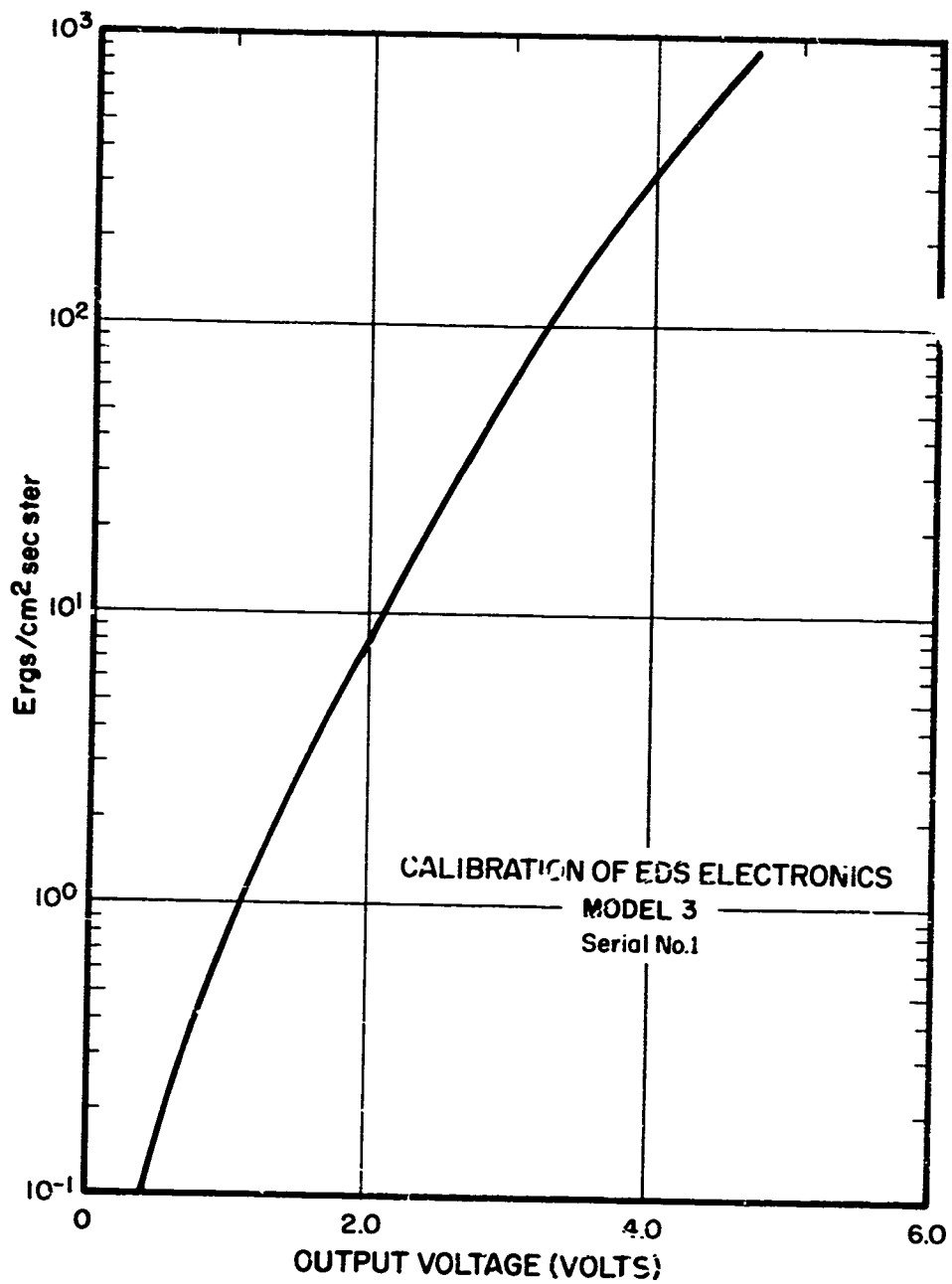


Fig. 13. Calibration curve for the energy deposition scintillator (Model 3, SN-1) on 17.750.

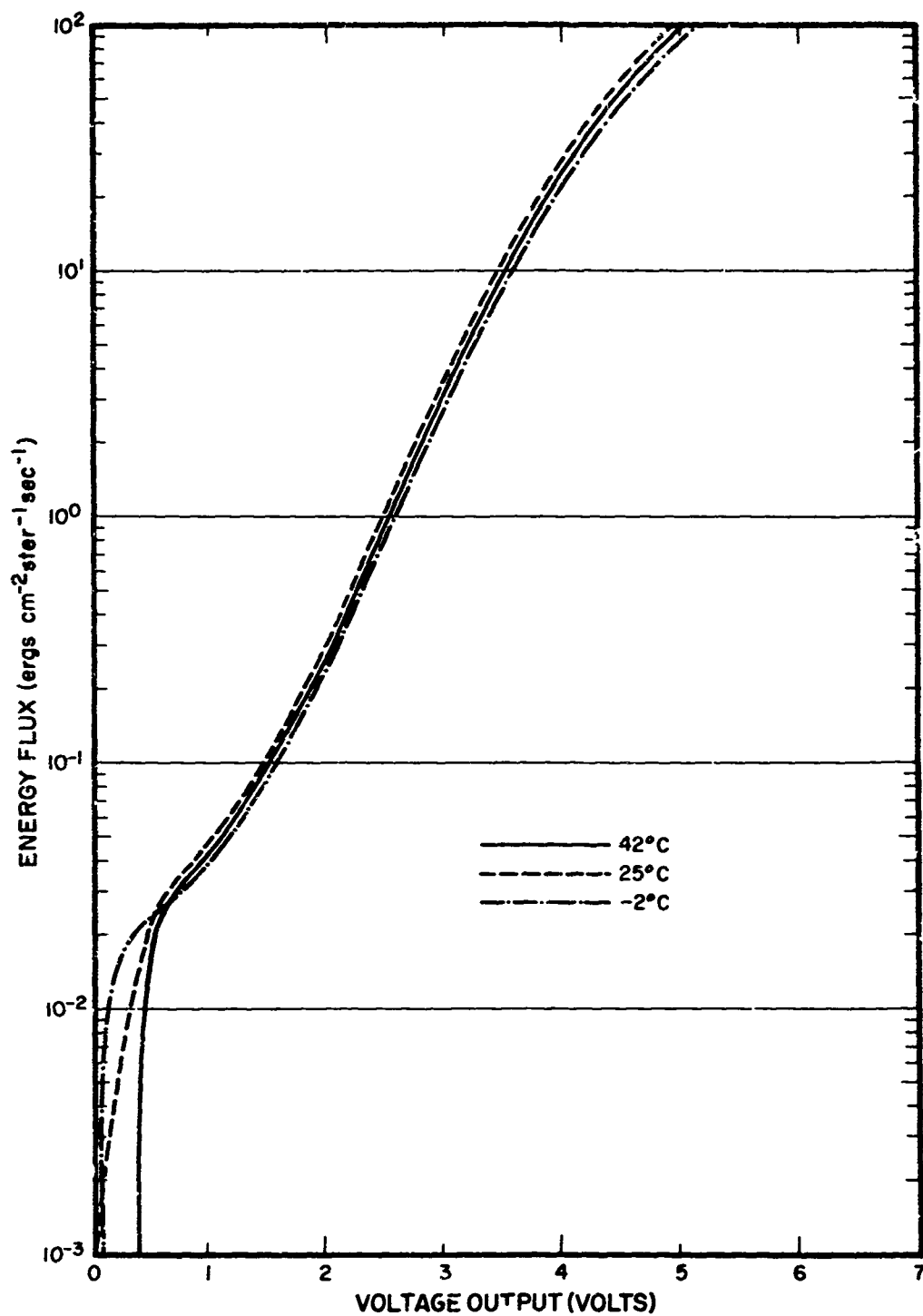


Fig. 14. Calibration curve for the energy deposition scintillator (Model 4, SN-1) on 17.751.

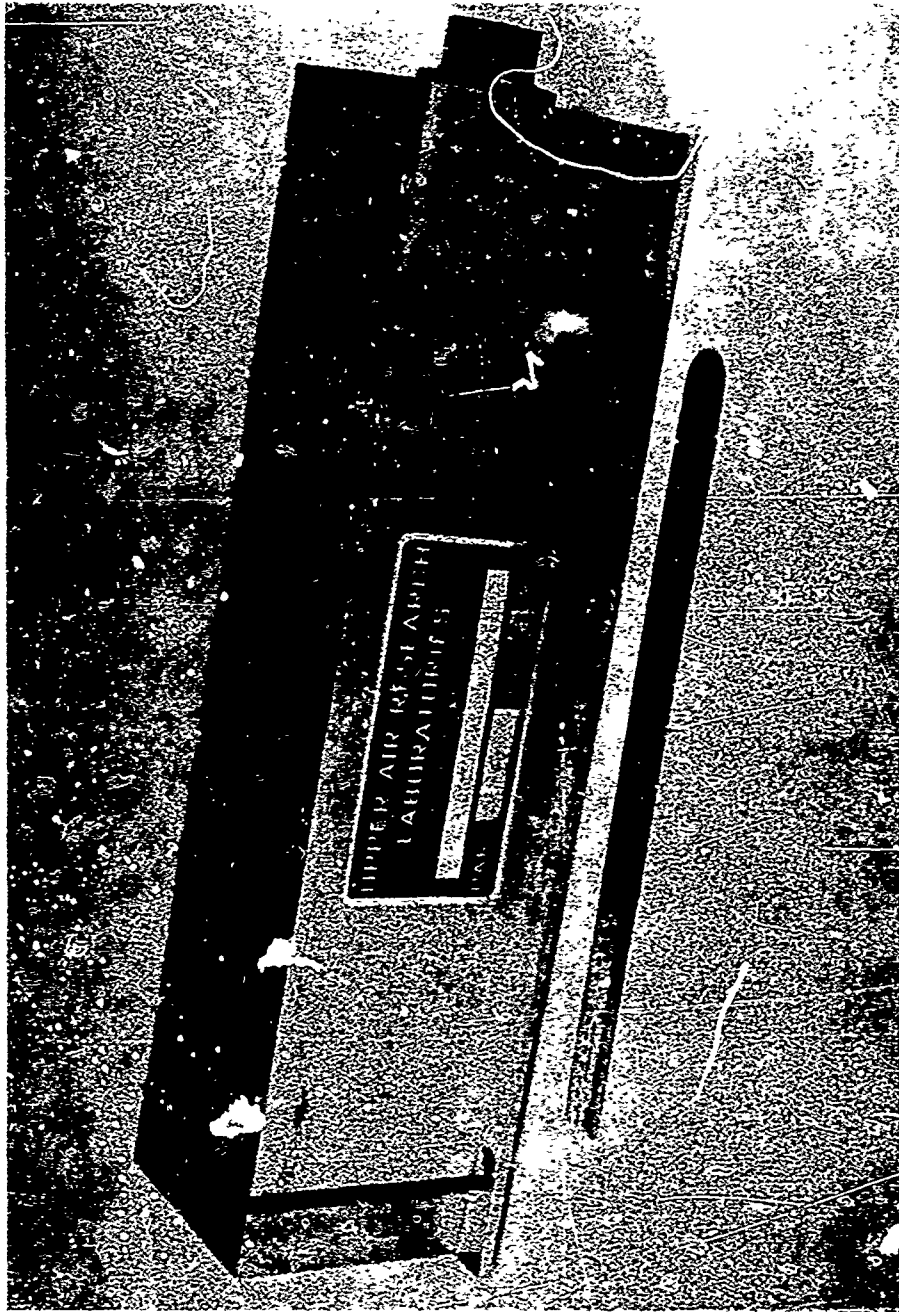


Fig. 15. Photograph of the Lyman- $\alpha$  detector.

For extended sources the proper equation is

$$i = \frac{I' A \Omega}{E}$$

$I'$  = irradiance in watts/cm<sup>2</sup> ster

$A \Omega$  = detector geometric factor in cm<sup>2</sup> ster

The chamber deteriorates rapidly when operated at currents higher than  $10^{-8}$  amp. For this reason the aperture area was set at 0.061 cm<sup>2</sup> to give a maximum chamber current of  $10^{-9}$  amp if the solar radiation is of the intensity expected. It was desirable to measure at least four orders of magnitude of energy; this made a very sensitive logarithmic amplifier necessary. The amplifier which was selected for 17.751 is shown in Figure 16; this amplifier was a slightly improved version of the one flown on 17.750. As shown, the input of the amplifier is an electrometer tube. The logarithmic characteristic is obtained by monitoring the screen-grid voltage required to hold the plate current constant for the different inputs. To give in-flight assurance that the amplifier was functioning correctly, a calibration circuit was installed at the input of the amplifier. This circuit consisted of 6.2 v applied through  $10^{10}$  ohms (for 20 msec at 20 sec intervals) to the input of the amplifier. Before the instrument is exposed, the chamber current will be zero; therefore, the output will be a short pulse of magnitude corresponding approximately to the  $6 \times 10^{-10}$  amp input. As the chamber current increases, the calibration pulse becomes less noticeable due to the logarithmic characteristics of the amplifier. A voltage monitor was included on the chamber voltage. The Lyman- $\alpha$  high voltage monitor calibration for 17.750 is shown in Figure 17; the high voltage monitor calibration for 17.751 was essentially the same. The Lyman- $\alpha$  system calibration for 17.750 is presented in Figure 18. Figure 19 shows the Lyman- $\alpha$  system calibration for 17.751. Complete lists of the characteristics for each unit are given in Table 7.



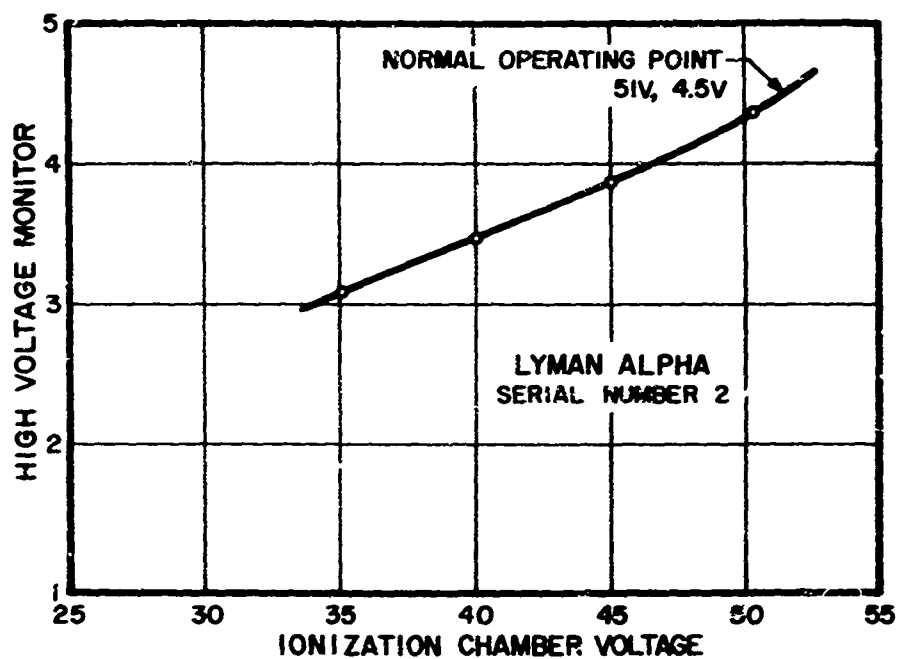


Fig. 17. High voltage monitor calibration for the 17.750 Lyman- $\alpha$  detector (Model La-67, SN-2). The 17.751 unit's calibration was essentially the same.

TABLE 7. Lyman- $\alpha$  detector characteristics

	17.750 Ly- $\alpha$ 67-2	17.751 Ly- $\alpha$ 67A-1
Field of view	30° full angle	30° full angle
Aperture area	0.0612 cm <sup>2</sup>	0.0612 cm <sup>2</sup>
Geometric factor	1.31 x 10 <sup>-2</sup> cm <sup>2</sup> ster	1.31 x 10 <sup>-2</sup> cm <sup>2</sup> ster
Chamber quantum efficiency	36.5%	26.7%
Chamber no.	M 1937	M 1940

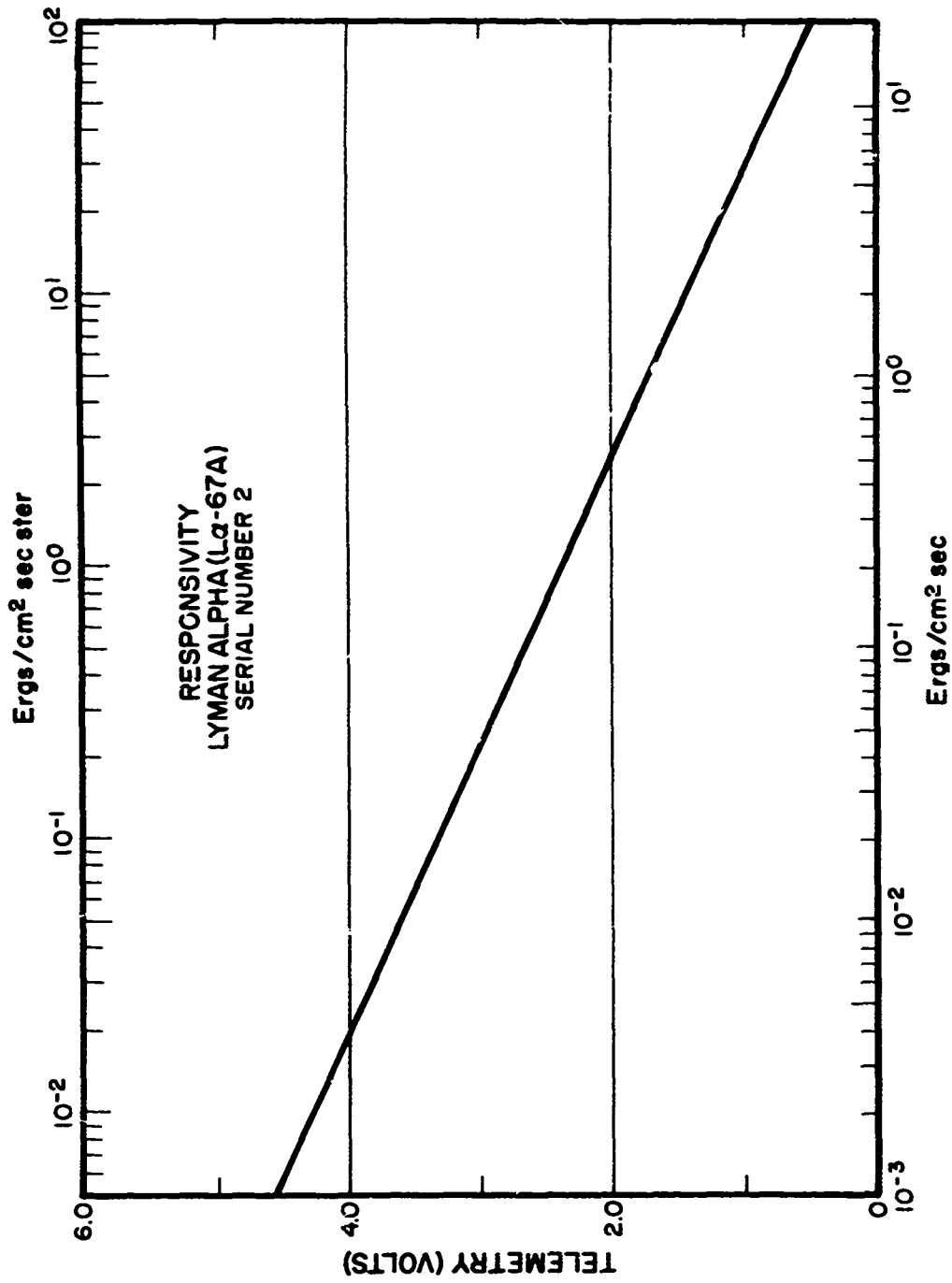


Fig. 18. System calibration of the 17.750 Lyman- $\alpha$  detector (Model L $\alpha$ -67, SN-2).

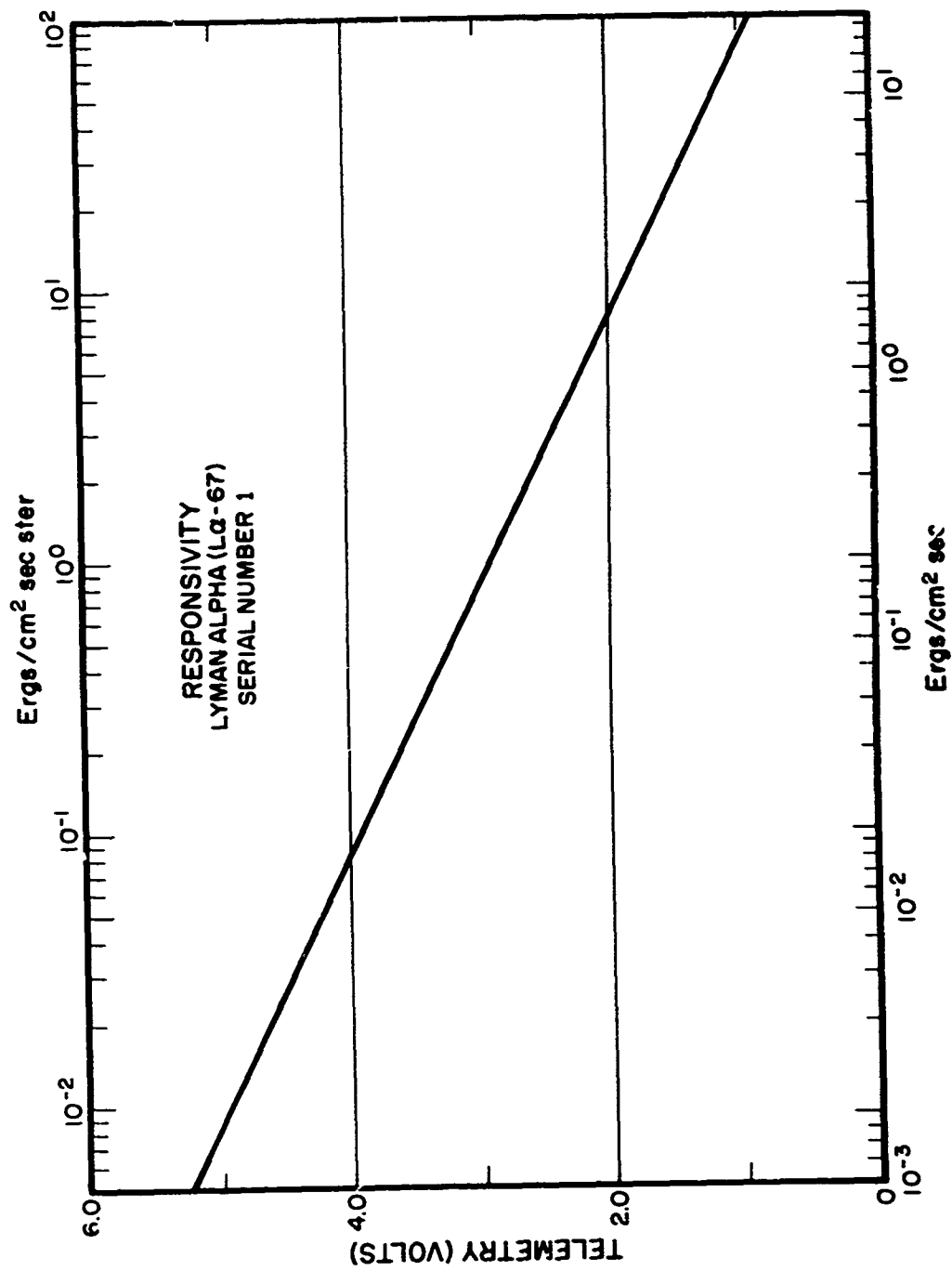


Fig. 19. System calibration of the 17.751 Lyman- $\alpha$  detector (Model L $\alpha$ -67A, SN-1).

### Langmuir Probe

A Langmuir probe was installed at the foremost point of the rocket on the tip of the nose spike antenna as shown in Figure 3. A photograph of the unit is shown in Figure 20. The collector surface was spherical with a radius of 3.175 cm, followed directly by a cylindrical guard electrode which was driven with the same potential as the collector.

There were two different model Langmuir probes flown on these two rockets. The most recently developed Langmuir probe was flown aboard 17.750, and one of the older models was flown on 17.751. The electronic circuitry in the older model has been reported in a previous paper on solar eclipse measurements [*Seljaas and Burt, 1967*]. The Langmuir probe on Black Brant 17.751 differed from the eclipse payloads in the packaging of the sweep oscillator which was modified to produce the sweep wave form shown in Figure 21 in order to measure further into the positive current region. The calibrations for 17.751 are shown in Figures 22 and 23 for electron and positive ion current regions, respectively.

The electronics in the unit which flew on 17.750 have also been reported in Scientific Report No. 1, "Langmuir probes for determining ionospheric particle densities and temperatures" [*Seljaas, 1968*]. The sweep voltage on this unit is given in Figure 24.

The illustration of the ion mode calibration for the Langmuir probe (17.750) is shown in Figure 25 while the electron mode is shown in Figure 26.

### Filter Wheel Photometer

The filter wheel photometer utilized a standard Utah State University model WT-1B [*Burt and Seljaas, 1966*] mated with a right angle mirror and a rotating filter wheel containing six one-inch diameter spike interference filters. The filters are changed by

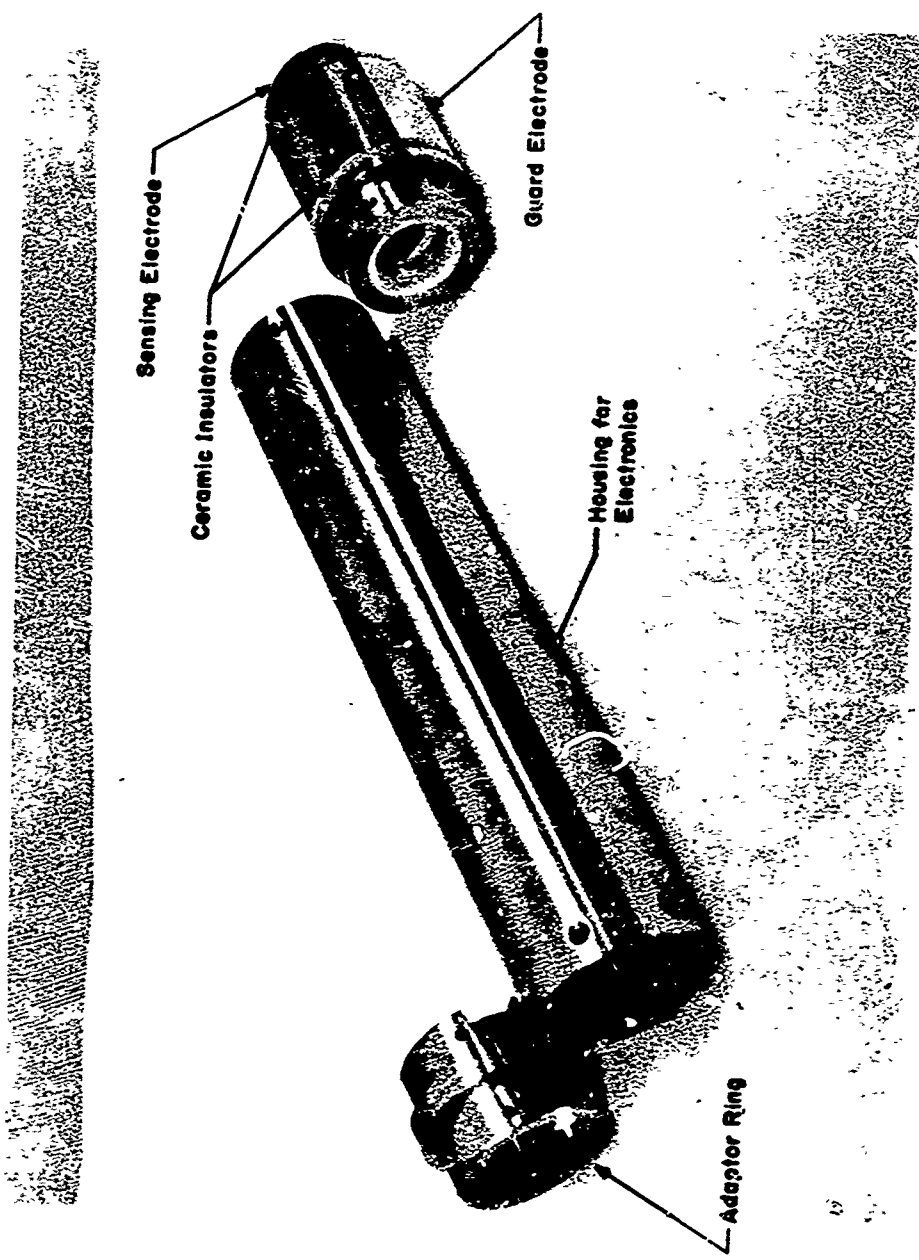


Fig. 20. Photograph of the 17.751 Langmuir probe.

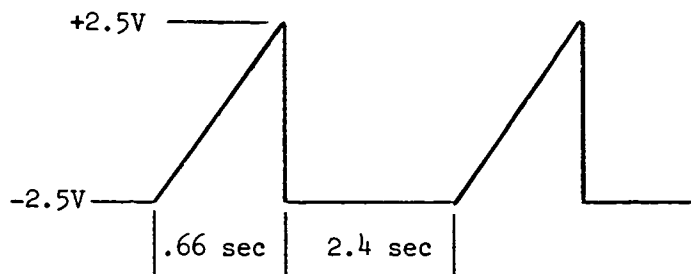


Fig. 21 Sweep wave form of the 17.751 Langmuir probe (Model B).

rotating the wheel continuously at 5 rps giving measurements at six different spectral regions 5 times per second. A picture of the completed photometer is shown in Figure 27. The mount was designed to allow the instrument to slide out through a door in the skin so that the mirror would provide a vertical look direction. After due consideration, it was feared that the instrument would be sensitive to scattered light from the tip of the nose spike on the rocket; therefore, the inboard half of the circular field of view was blocked. This gave a final field of view of a semicircle having a solid angle of 0.015 steradians. The general instrument specifications are contained in Table 8 for 17.750 and Table 9 for 17.751. A complete set of responsivity calibrations for each filter is given in Figures 28a, 28b, and 28c, for 17.750; and in Figures 29a, 29b, and 29c, for 17.751.

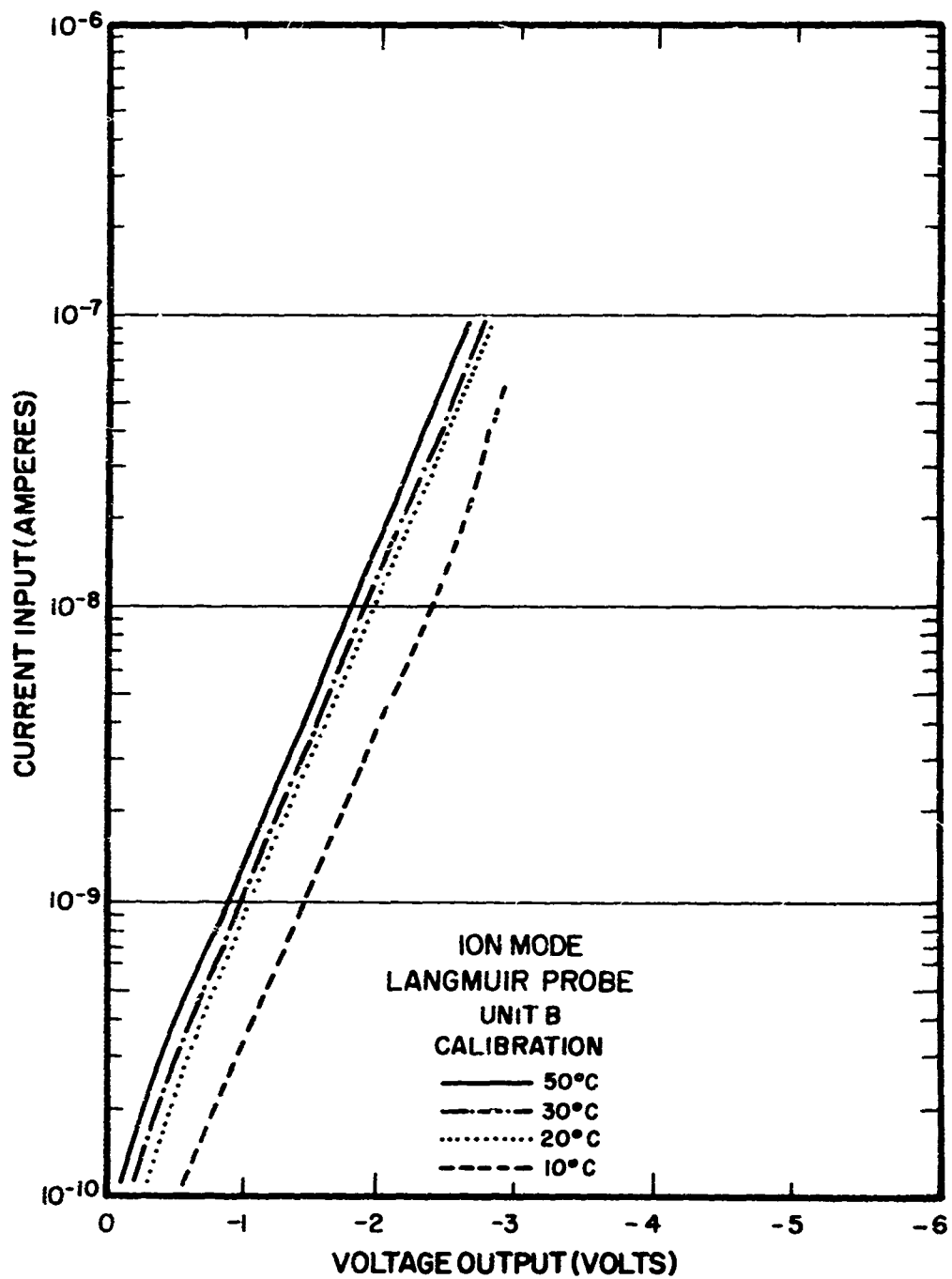


Fig. 22. Ion mode calibration of the 17.751 Langmuir probe (Model B).

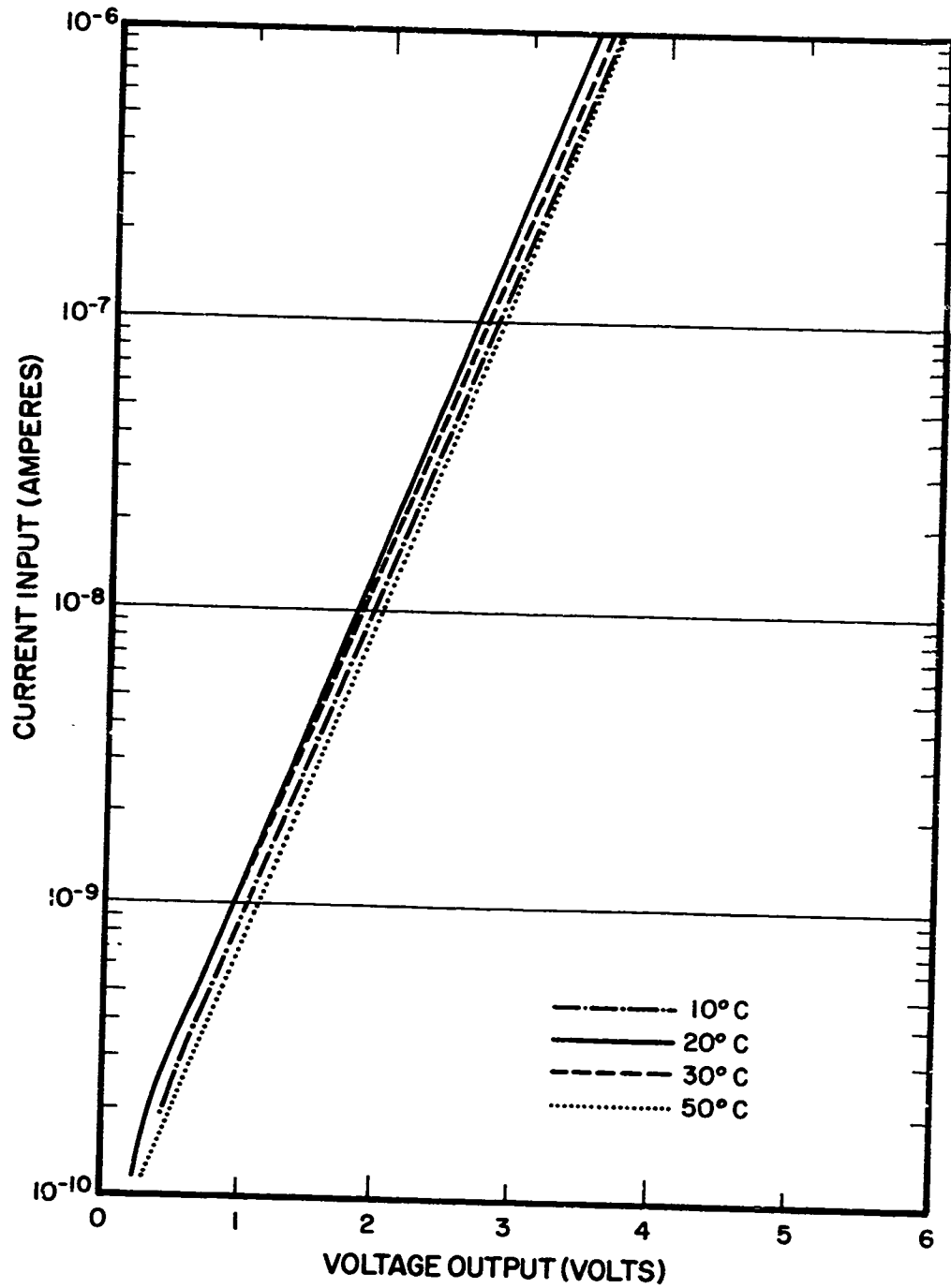


Fig. 23. Electron mode calibration of the 17.751 Langmuir probe (Model B).

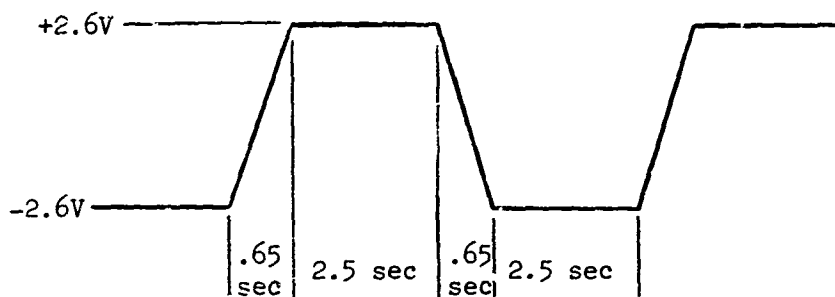


Fig. 24. Sweep wave form of the 17.750 Langmuir probe (Model LP-67-C, SN-1).

TABLE 8. Specifications for Filter Wheel Photometer, Model WT 1-B, SN 22-FW-1 (17.750)

Filter	Center Wavelength, A	Bandwidth ( $\Delta\lambda$ ), A	Transmission at Peak, %	Maximum Measurable Signal, kR	Minimum Measurable Signal, R
1	3921	42	21	170	24
2	5573	45	63	245	175
3	5770	135	55	362	217
4	4861	60	63	122	30
5	4020	40	23	126	50
6	3800	36	14	117	60

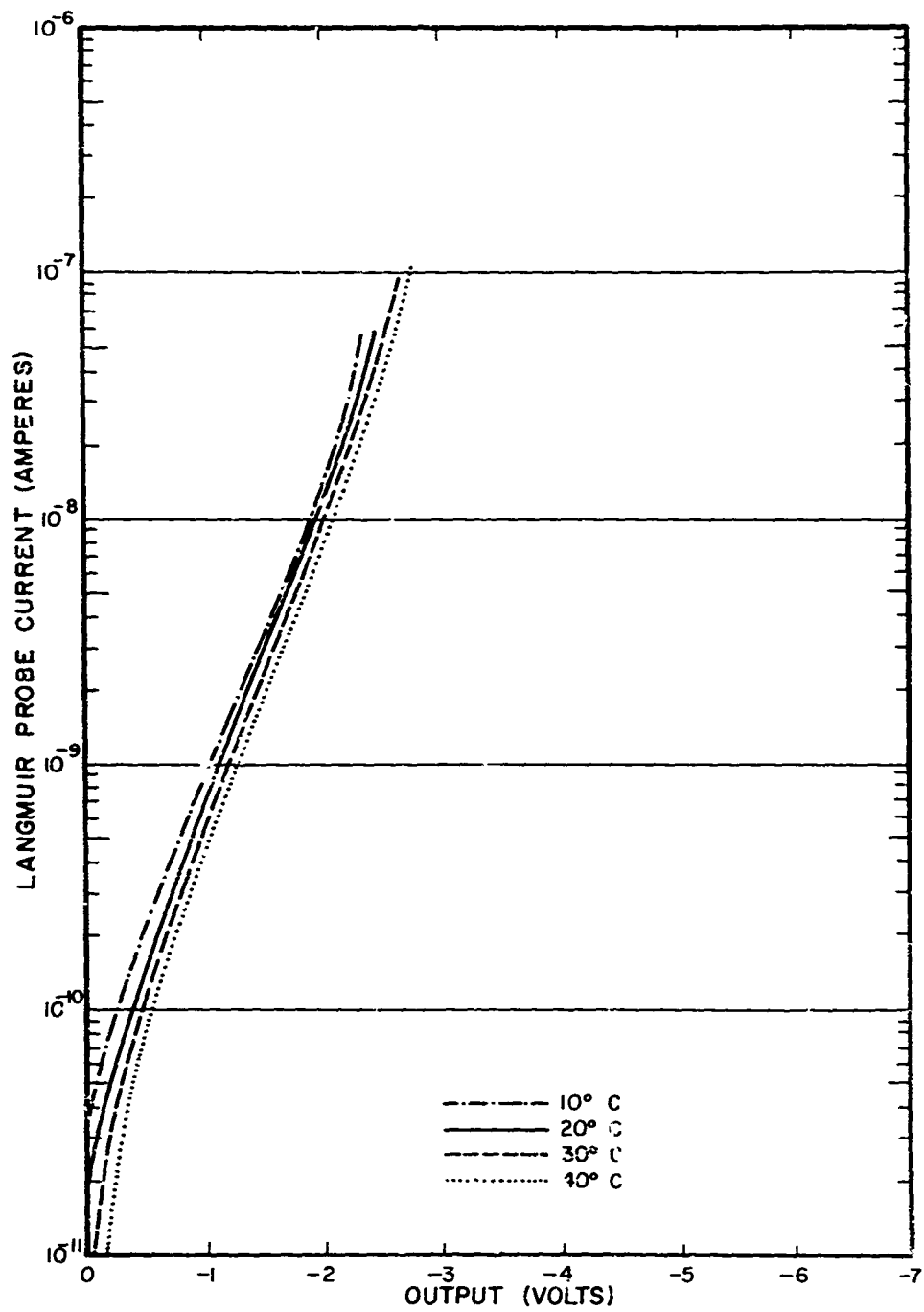


Fig. 25. Ion mode calibration of the 17.750 Langmuir probe (Model LP-67-C, SK-1).

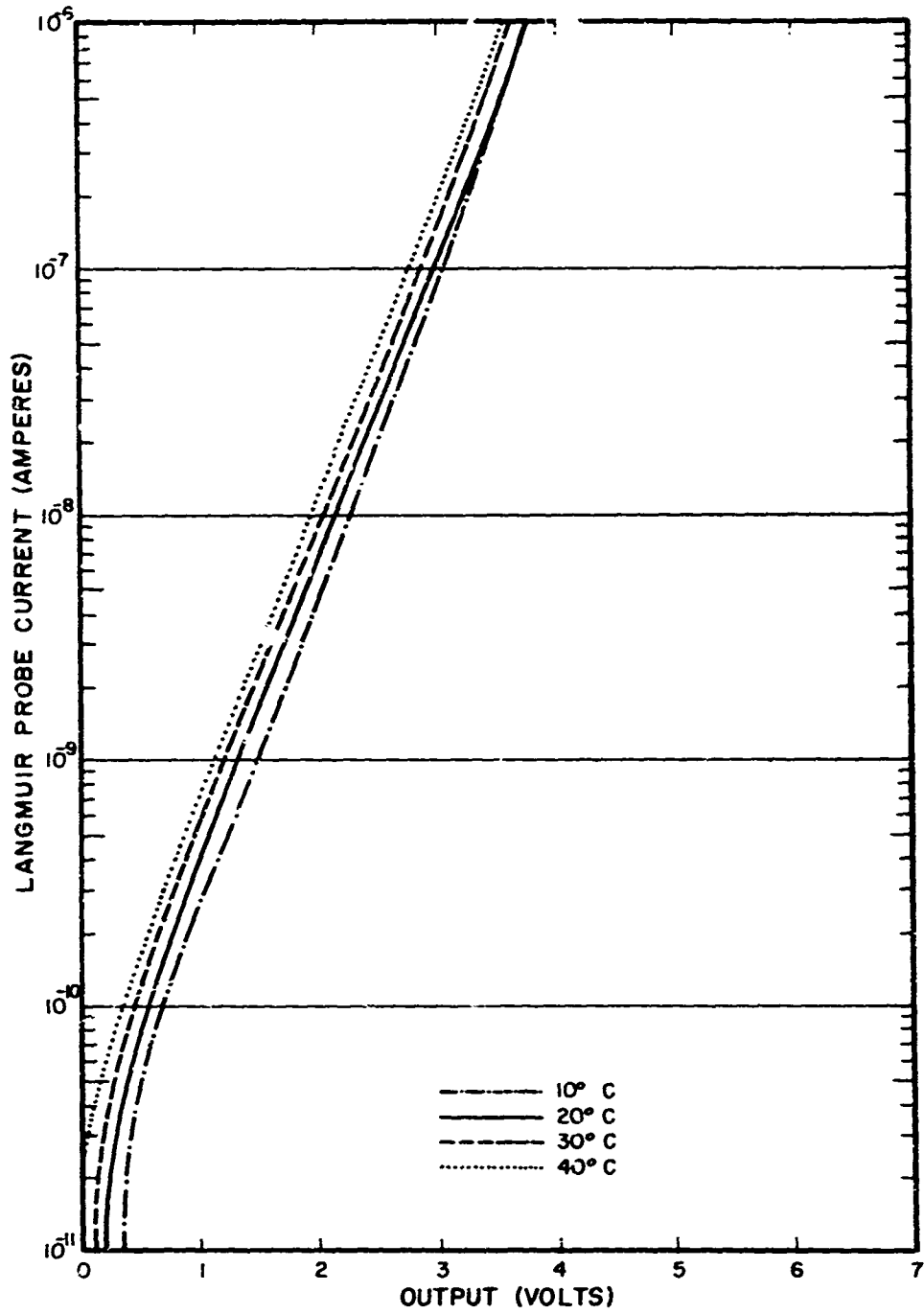


Fig. 26. Electron mode calibration of the 17.750 Langmuir probe (Model LP-67-C, SN-1).

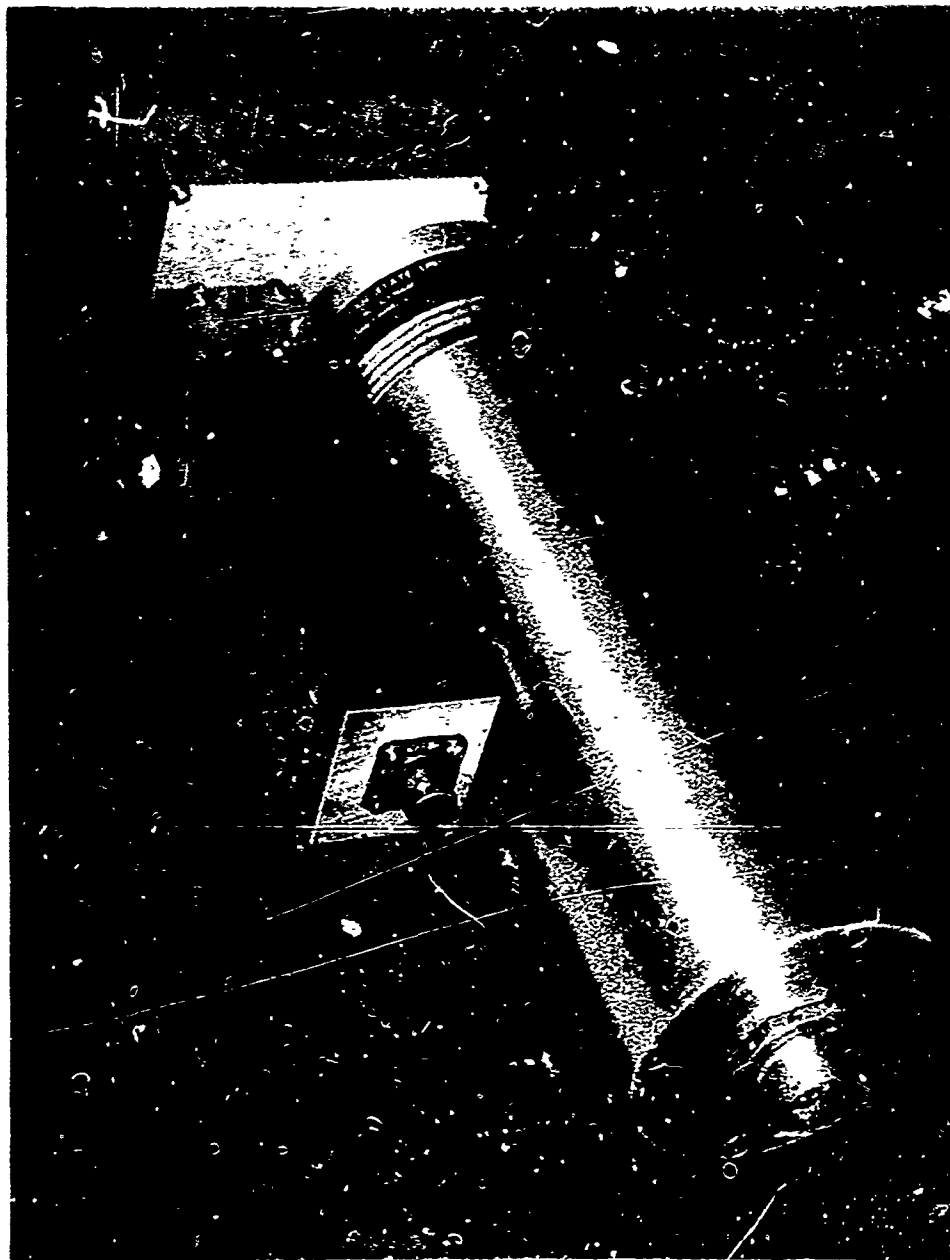


Fig. 27. Photograph of the filter wheel photometer.

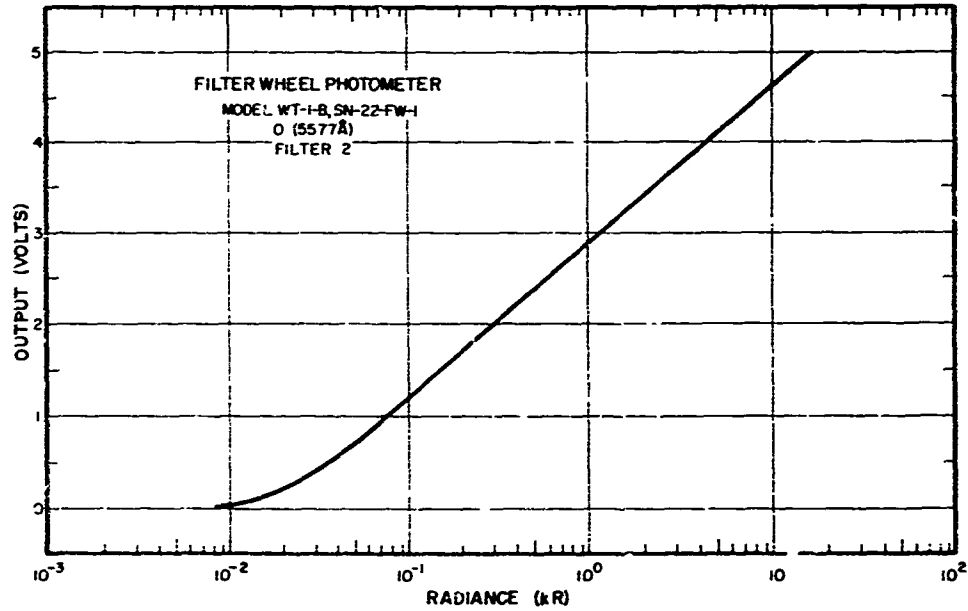
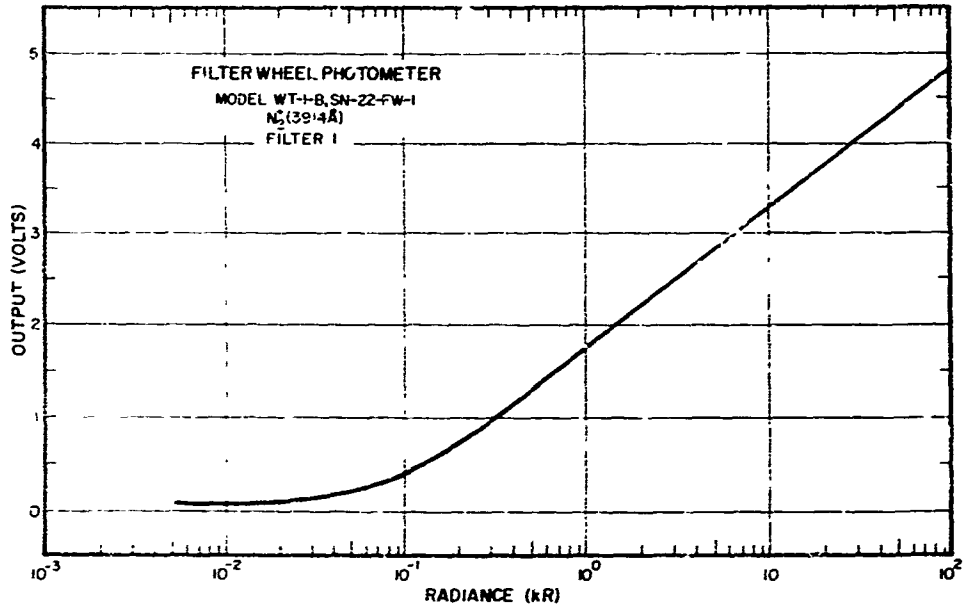


Fig. 28a. Responsivity calibrations for filters 1 and 2 of the 17.750 filter wheel photometer (Model WT-1-B, SN-22-FW-1).

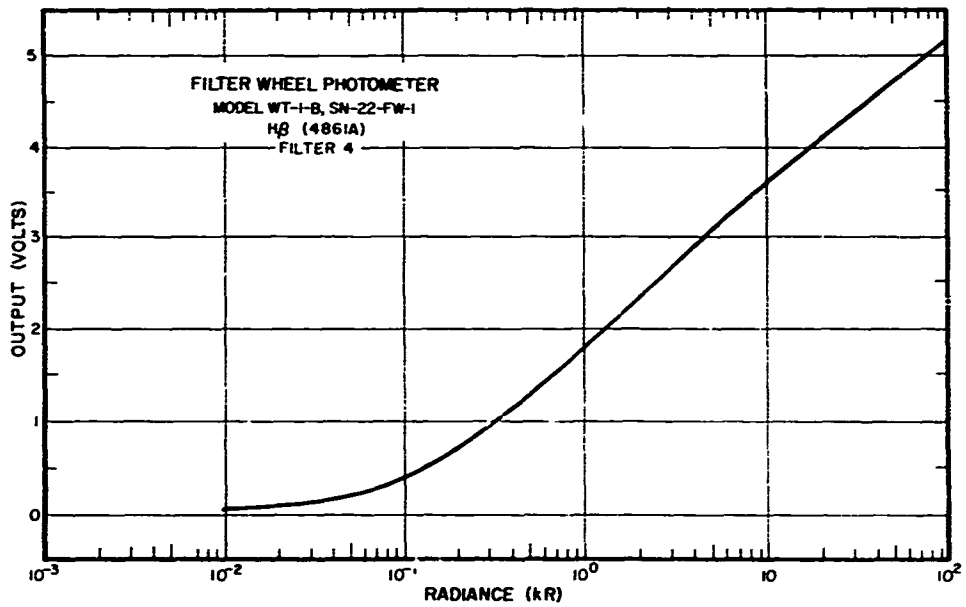
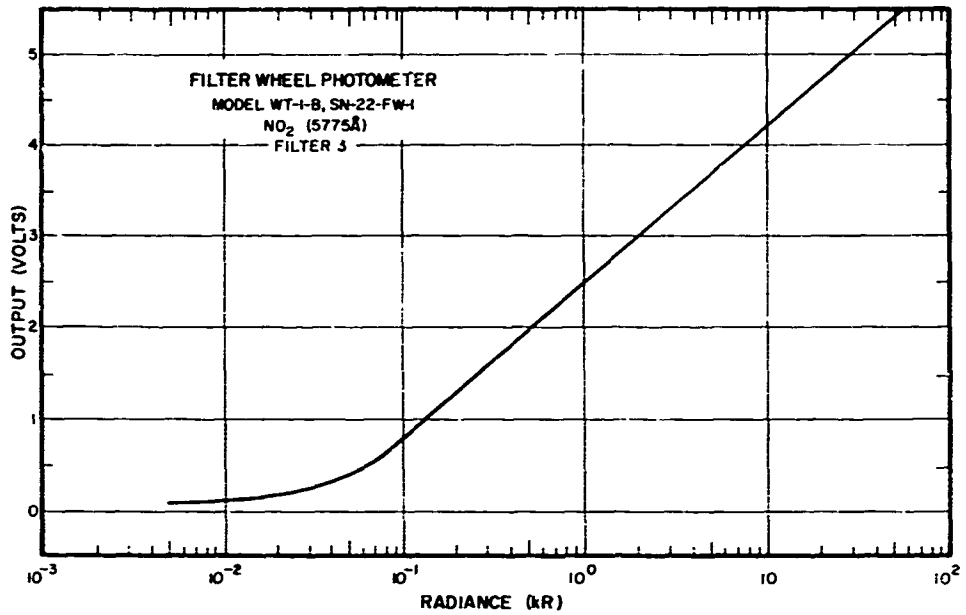


Fig. 28b. Responsivity calibrations for filters 3 and 4 of the 17.750 filter wheel photometer (Model WT-1-B, SN-22-FW-1).

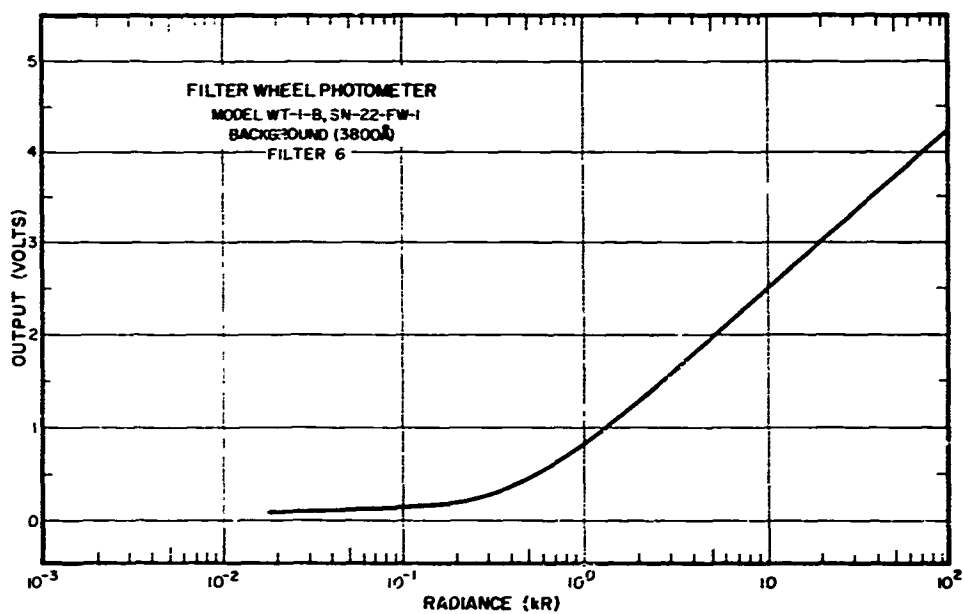
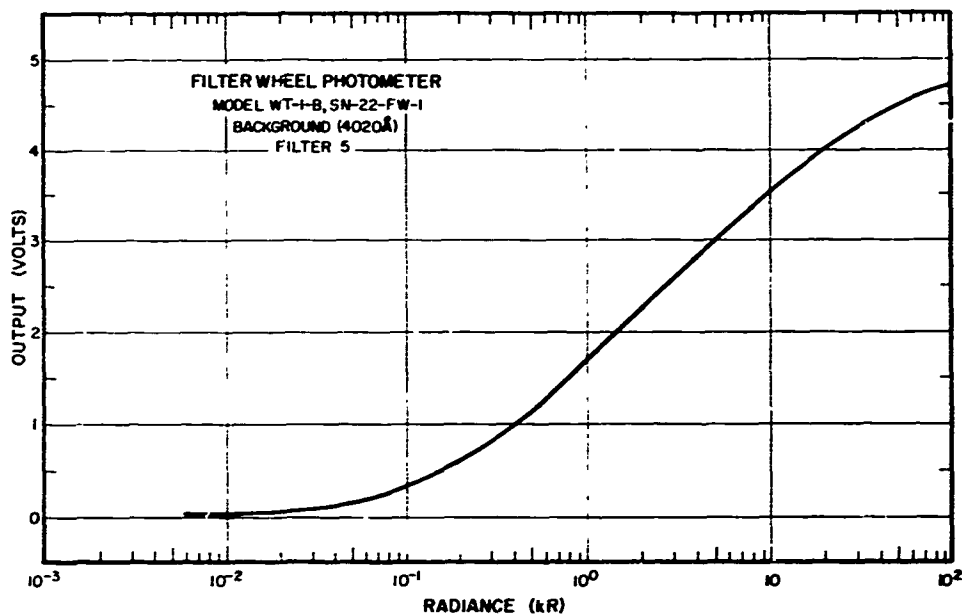


Fig. 28c. Responsivity calibrations for filters 5 and 6 of the 17.750 filter wheel photometer (Model WT-1-B, SN-22-FW-1).

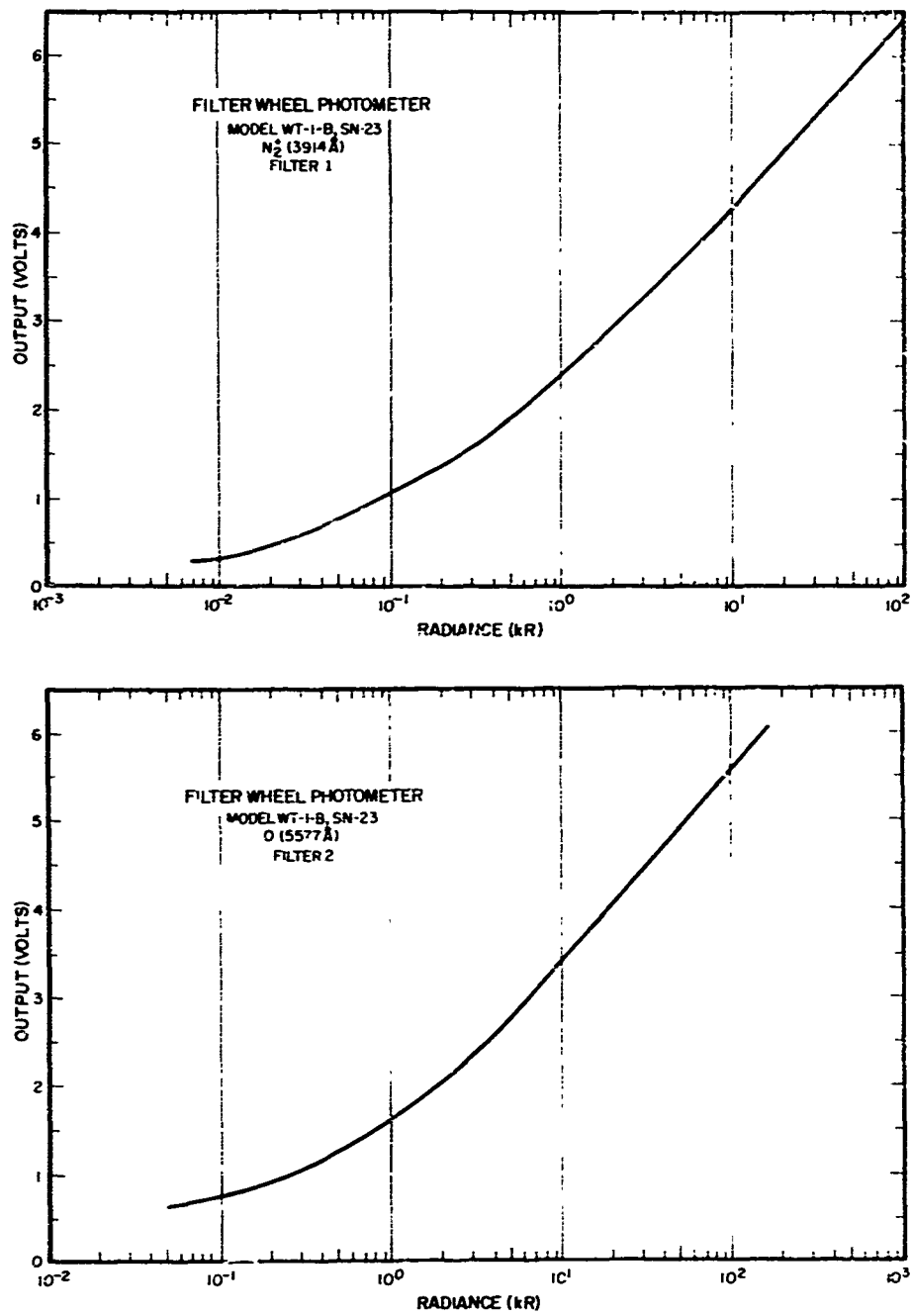


Fig. 29a. Responsivity calibrations for filters 1 and 2 of the 17.751 filter wheel photometer (Model WT-1-B, SN-23).

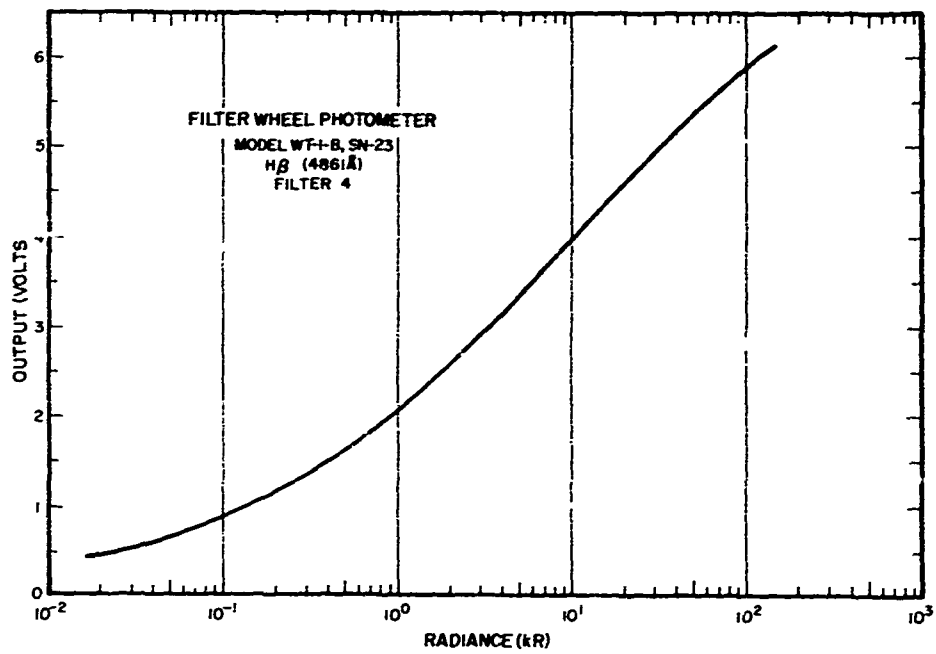
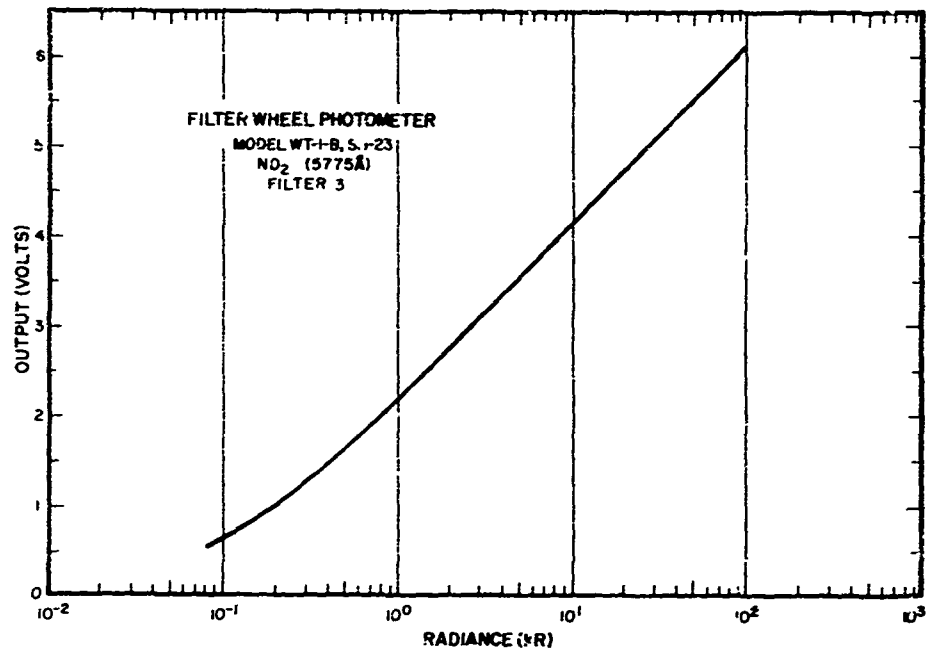


Fig. 29b. Responsivity calibrations for filters 3 and 4 of the 17.751 filter wheel photometer (Model WT-1-B, SN-23).

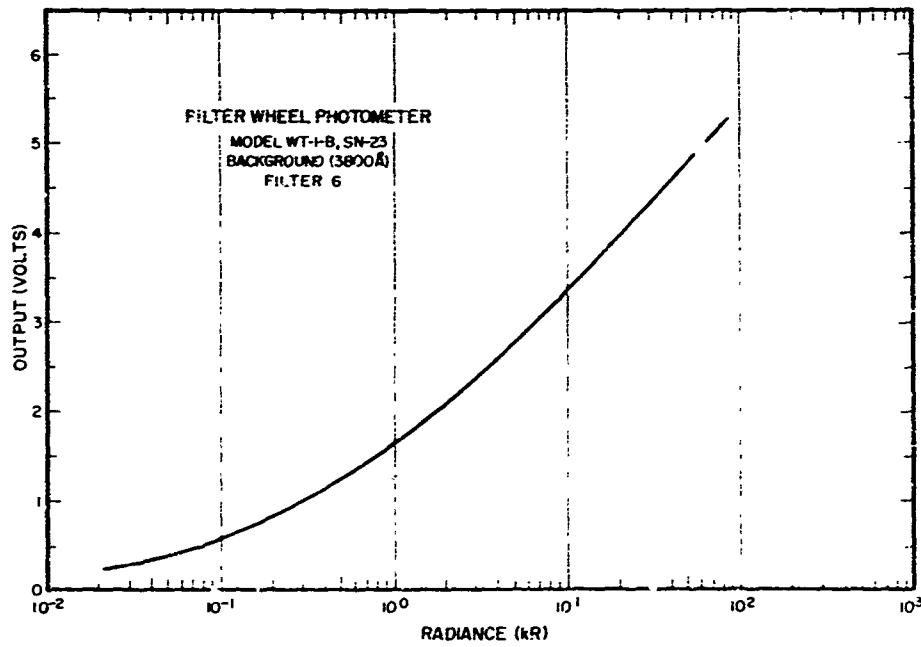
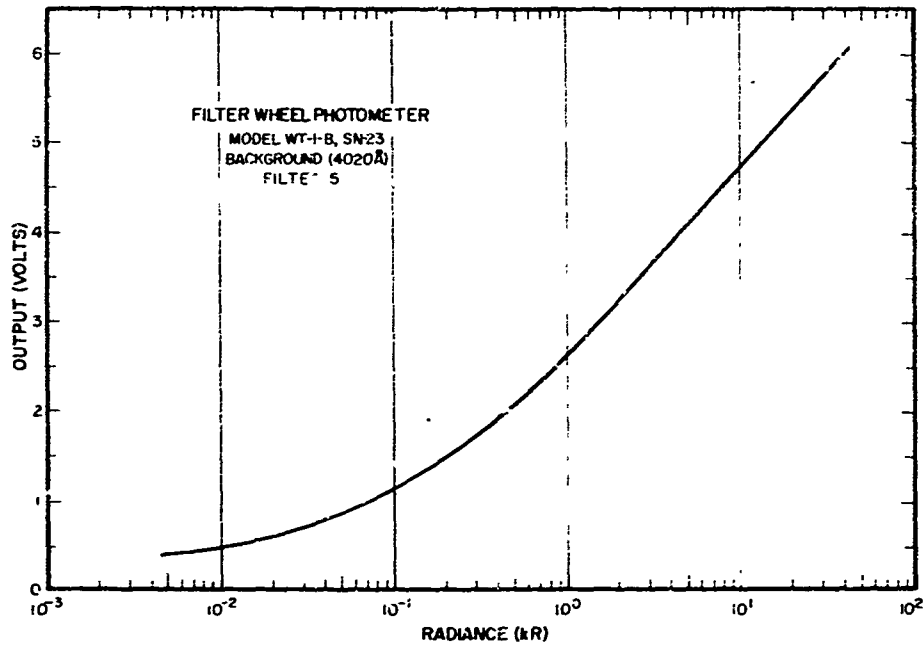


Fig. 29c. Responsivity calibrations for filters 5 and 6 of the 17.751 filter wheel photometer (Model WT-1-B, SN-23).

TABLE 9. Specifications for Filter Wheel Photometer  
Model WT-1-B, SN-23 (17.751).

Filter	Center Wavelength, A	Bandwidth ( $\Delta\lambda$ ), A	Transmission at Peak, %	Maximum Measurable Signal, kR	Minimum Measurable Signal, R
1	3921	42	21	25	8
2	5573	45	63	52	17
3	5770	135	55	58	73
4	4863	60	63	3	2
5	4020	40	23	15	8
6	3800	36	14	48	96

The calibration curve for the high voltage monitor is shown in Figure 30, and the calibration curve for the temperature monitor is shown in Figure 31. Complete information on the optical characteristics of each filter is given in Appendix B.

#### Telemetry System

The Black Brants 17.750 and 17.751 each contained two 4 watt FM telemetry links operating at carrier frequencies of 234 MHz (link 1) and 246.3 MHz (link 2). The telemetry subcarrier assignments are given in Tables 10 and 11, and the commutator data assignments are listed in Table 12.

#### Trajectory and Aspect Systems

The aspect of the two rockets was determined by a MARS gyro system, and each had a magnetometer to give the direction of the magnetic field. The position of the magnetometer and the gyro notch are shown in Figure 2. The trajectory was determined by the range radar and a beacon on the rocket.

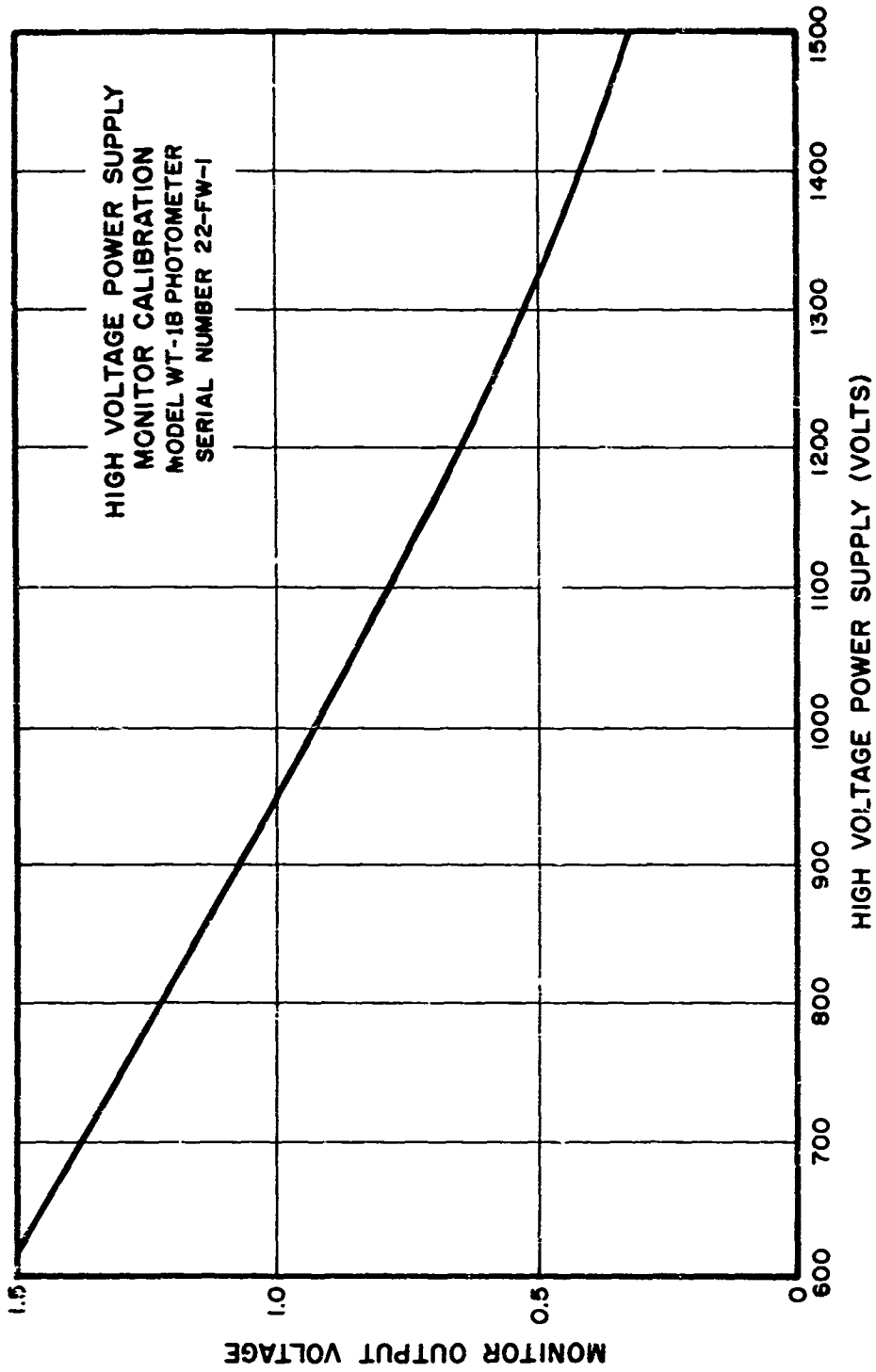


Fig. 30. High voltage monitor calibration curve for the filter wheel photometer (Model WT-1-B, SN-22-FW-1) on 17.750.

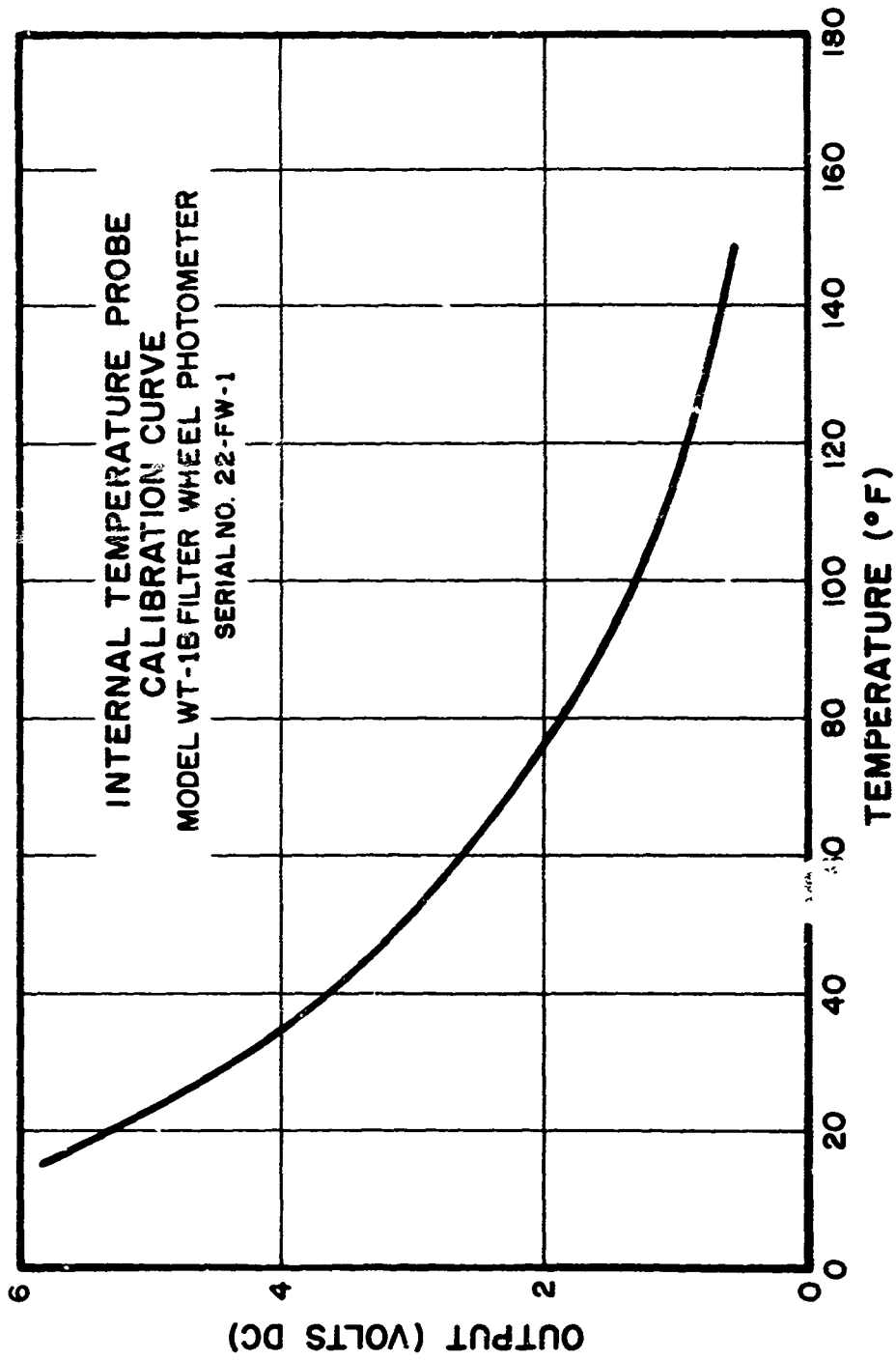


Fig. 31. Temperature monitor calibration curve for the filter wheel phot. ex (Model WT-1-B, SN-22-FW-1) on 17.750.

TABLE 10. Black Brants 17.750 and 17.751 Telemetry Assignments, Link 1 (234 MHz)

IRIG Channel	Frequency (KHz)	Data Description
18	70.0	Particle spec. pulse (Panametrics)
17	52.5	X-ray pulse train (Utah)
16	40.0	Langmuir probe (Utah)
15	30.0	SWIP Commutator - 5 x 30 IRIG (Utah)
14	22.0	Commutator - 2.5 x 30 IRIG (CREK)
13	14.5	Aspect Gyro Multiplexer (CREK)
12	10.5	Photometer (Utah)
11	7.35	Propagation (Penn. State)
10	5.4	Propagation (Penn. State)
9	3.9	Lyman- $\alpha$ (Utah)
8	3.0	Scintillator (Utah)
7	2.3	Langmuir probe (Utah)
6	1.7	SWIP Ant. Vo 1 - 17.750 (Utah)* Z $\theta$ Probe - 17.751 (Utah)
5	1.3	D.C. Conductivity (Penn. State)

\* The change of assignment on channel 6 constituted the only difference in the two payloads' telemetry assignments.

TABLE 11. Black Brants 17.750 and 17.751 telemetry assignments, Link 2 (246.3 MHz)

IRIG Channel	Frequency (KHz)	Data Description
18	70.0	Particle spect. pulse (Panametrics)
17	52.5	Conductivity probe (Penn. State)
16	40.0	Conductivity probe (Penn. State)
15	30.0	R.P.A. (Adcole)
14	22.0	Gerdian (+) boom (Adcole)
13	14.5	Gerdian (-) body (Adcole)
12	10.5	Gerdian (+) body (Adcole)
11	7.35	Gerdian boom sweep (Adcole)
10	5.4	Gerdian condenser sweep (Adcole)
9	3.9	R.P.A. sweep (Adcole)
8	3.0	Accelerometer - long axis (CREK)
7	1.7	Magnetometer - roll (CREK)
6	1.3	D.C. conductivity (Penn. State)

TABLE 12. Commutator Data Assignments for Black  
Brants 17.750 and 17.751

Channel	Data	Experimenter
Datametrics 949A	Frame Sync Pulse +5 V Channel Sync (Pedestal) -1.25 V	2 1/2 x 30 IRIG
1	Zero (0) volt calibration	CREK
2	(+) 3 volt monitor	Panametrics
3	(+) 4 volt monitor	Panametrics
4	Photometer temperature	Utah
5	Photometer high voltage	Utah
6	Scintillator temperature	Utah
7	Not used for data	
8	Not used for data	
9	Lyman- $\alpha$ high voltage	Utah
10	Not used for data	
11	Not used for data	
12	Not used for data	
13	Not used for data	
14	Not used for data	
15	Te monitor	Adcole
16	Tg-3 monitor	Adcole
17	Tg-2 monitor	Adcole
18	Tg-1 monitor	Adcole
19	(+) 1 volt monitor	Panametrics
20	Not used for data	
21	Door No. 1 release monitor	CREK
22	Door No. 2 release monitor	CREK
23	Door No. 3 release monitor	CREK
24	Door No. 4 release monitor	CREK
25	Boom meter monitor	CREK
26	Photometer extend monitor	Utah
27	Gerdian boom extend monitor	Adcole
28	R.P.A. boom extend monitor	Adcole

## RESULTS AND CONCLUSION

Due to the sparsity of PCA events in 1967 it was decided to fly the first Black Brant (17.750) into an auroral absorption event during December, 1967 to test fly the rocket configuration and the instruments for the PCA program.

Black Brant 17.750 was launched Wednesday, 6 December 1967, at 10:14:51.46 from Churchill Research Range during an auroral absorption event of about 2 db of 30 MHz absorption.

The rocket performed well achieving an apogee of 135 km with a roll rate (after extension of booms) of 1.9 per second with a precession cone of  $1.5^\circ$  half angle. The altitude plot is shown in Figure 32.

All instruments except the propagation experiment provided data which are being analyzed and will be reported elsewhere.

During the field trip when 17.750 was fired the second Black Brant (17.751) was put into complete readiness and placed in standby condition to await the occurrence of a PCA event. Instructions were prepared so that Churchill Research Range personnel could install batteries and launch the rocket when such an event occurred. On 10 June 1968 a PCA event developed and the rocket was launched. Approximately 10 seconds after launch, the rocket broke up due to abnormal flight dynamics. A closeup picture of the remaining carcass of 17.751 is shown in Figure 33.

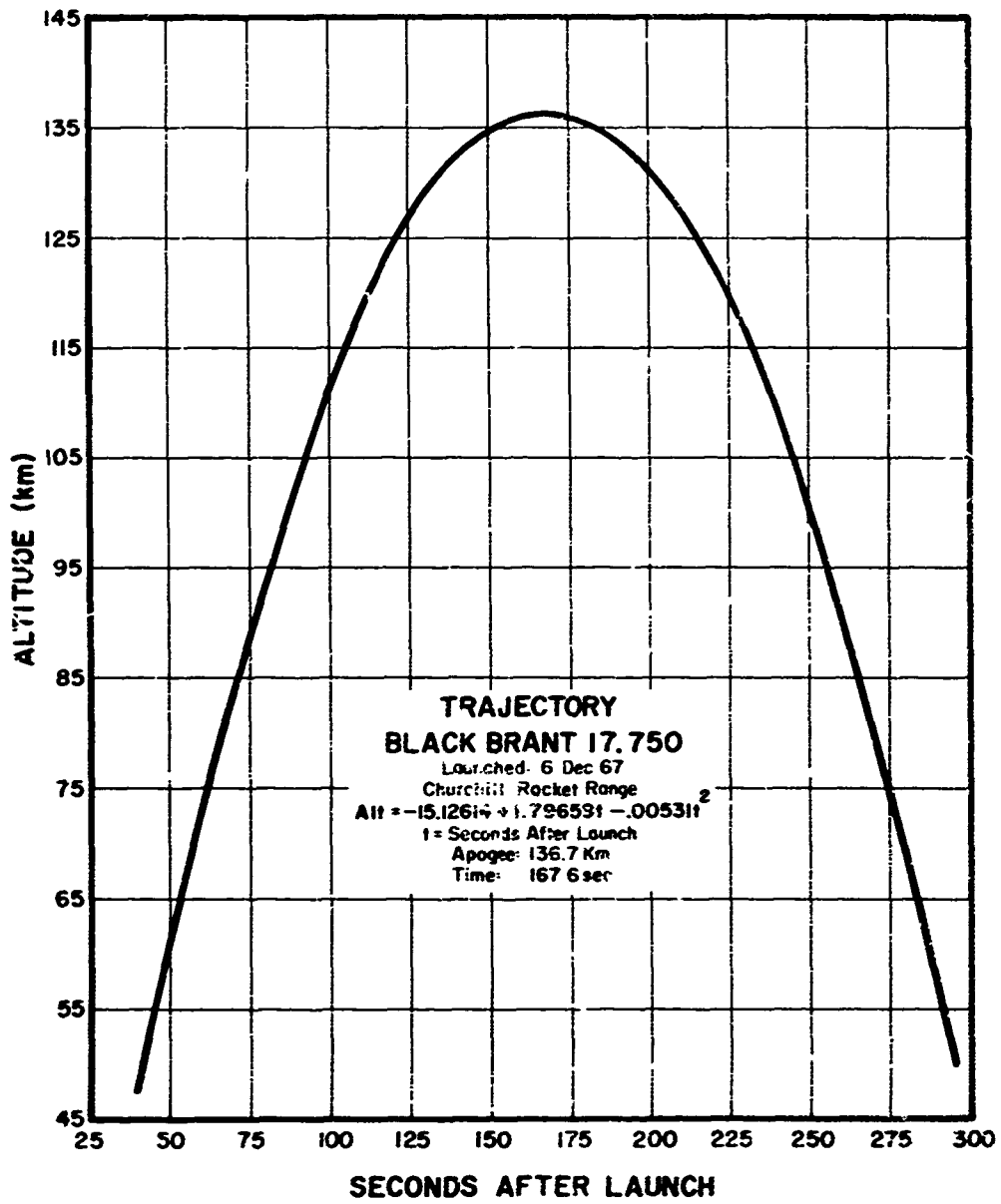


Fig. 32. Trajectory of Black Brant 17.750.



Fig. 33. Picture of the recovered payload of Black Brant 17.751. The payload separated due to the abnormal flight dynamics of the rocket.

APPENDIXES

APPENDIX A

Impedance Probe Experiment Information  
and Calibration Data (17.750)

GENERAL INFORMATION

Vehicle code no.:	Black Brant 17.750
Electronics box code no.:	11119-98
Experiment type:	SWIP
Experiment frequencies:	3.0 MHz            7.2 MHz
Tuned antenna impedance:	19 + j51 ohms    70 + j66 ohms
Shunt capacitance:	43 pf
R.F. cable information	
A. Type:	178 BU
B. Lengths internal to experiment box:	13.3 cm
C. Lengths external to experiment box:	8.4 cm
D. Total lengths:	21.7 cm

CALIBRATION INFORMATION

Laboratory checkout

A. Persons responsible:	G.S. Hale
B. Date:	January 1967
C. Form of calibration data:	Visicorder
D. Present data location:	Upper Air Research Laboratory
E. Electronics box weight:	6.6 lb with network
F. Current drain:	250 ma
G. Voltage:	28V

LINE CALIBRATION INFORMATION

Simulated telemetry load: 470K

Calibration box

- A. No. 1 for 3 MHz
- B. No. 2 for 7.2 MHz

RF voltage level at antenna jacks

- A. .7V P.P. at 7.2 MHz
- B. .8V P.F. at 3 MHz

CIRCUIT BOARDS

Name	Model and Serial No.
Commutator line	CEL 11105 5 MHz
Commutator reference voltage	CEL 11105
Oscillating mute switch	
Oscillating switch driver	CEL 11073 M-1
3 MHz oscillator	CEL 11108 M-3
Oscillating switch	
7.2 MHz oscillator	CEL 11072 M-1

Transmission Line RF Measurements HP410C

Assigned to Probe No. 17.75C BB, Line No. CI 5-109

Output Voltage from Generator 1.12

Operator - G.S. Hale, 12 January 1966

PIN NO. (Numbered from osc end)	Freq. 7.2 MHz		Freq. 7.2 MHz		Freq. 3 MHz	
	Short	50 $\Omega$	Short	50 $\Omega$	Short	50 $\Omega$
1	1.12	0.488	1.13	1.39	1.33	1.30
2	1.53	0.484	1.44	1.38	1.44	1.298
3	1.81	0.480	1.72	1.37	1.56	1.29
4	1.98	0.479	1.88	1.37	1.68	1.28
5	2.03	0.479	1.94	1.37	1.76	1.28
6	1.94	0.479	1.86	1.37	1.83	1.28
7	1.72	0.481	1.68	1.37	1.87	1.28
8	1.40	0.479	1.38	1.37	1.89	1.28
9	0.97	0.477	1.02	1.36	1.90	1.275
10	0.48	0.473	0.51	1.35	1.88	1.275
11	0.03	0.468	0.15	1.33	1.85	1.275
12	0.24	0.462	0.36	1.32	1.81	1.275
13	0.75	0.458	0.82	1.31	1.74	1.275
14	1.23	0.457	1.22	1.31	1.64	1.275
15	1.63	0.458	1.56	1.31	1.53	1.273
16	1.89	0.462	1.82	1.32	1.39	1.272
17	2.05	0.468	1.95	1.33	1.26	1.270
18	2.07	0.473	1.98	1.34	1.11	1.270
19	1.97	0.480	1.88	1.36	0.94	1.260
20	1.75	0.484	1.70	1.37	0.77	1.260
21	1.40	0.487	1.38	1.38	0.59	1.251
22	0.95	0.485	1.01	1.39	0.39	1.243
23	0.46	0.479	0.58	1.38	0.21	1.240
24	0.01	0.472	0.13	1.37	0.00	1.230

Transmission Line Bridge Measurements

Assigned to Probe No. 17.750, Black Brant. Line No. CL-5

Operator - G.S. Hale, 11 January 1969

Calibration Check Freq.	7.2 MHz		3.0 MHz	
	OSC End	Ant End	OSC End	Ant End
$Z_c$ C	13 + j9.6	13 + j9.9	6.5 + j17	6.5 + j18
	13 + j9.6	13 + j9.9	6.5 + j17	
$Z_s$ C	5 - j4.6	5.2 - j4.7	4.5 - j16	4.2 - j17
	5 - j4.6	5.2 - j4.7	4.5 - j16	4.2 - j17
$Z_{50}$ ohm	48 - j.20	49 - j.04	48 - j.67	49 - j.33
	48 - j.20	49 - j.04	48 - j.67	49 - j.33

Impedance Probe Experiment Information  
and Calibration Data (17.751)

GENERAL INFORMATION

Vehicle code no.:	Black Brant 17.751	
Experiment type:	ZOP and SWIP	
Experiment frequencies:	3 MHz	7.2 MHz
Tuned antenna impedance:	24 + j53 ohms	71 + j68 ohms
Antenna shunt capacitance:	49.6 pf	
R.F. cable information		
A. Type:	178 BU	
B. Lengths internal to experiment box:	14.2 cm	
C. Lengths external to experiment box:	9.0 cm	
D. Total lengths:	23.2 cm	

CALIBRATION INFORMATION

Laboratory checkout

A. Persons responsible:	G.S. Hale
B. Date:	September 1967
C. Form of calibration data:	Visicorder and tables
D. Present data location:	Upper Air Research Laboratory
E. Electronics box weight:	6.6 lb with network
F. Current drain:	375 ma
G. Voltage:	28V

LINE CALIBRATION INFORMATION

Simulated telemetry load: Visicorder input

Calibration box

A. No. 1 for 3 MHz

B. No. 2 for 7.2 MHz

RF voltage level at antenna jacks

A. .7V rms P.P. at 3 MHz

B. .7V rms P.P. at 7.2 MHz

Transmission Line RF Measurements

Assigned to Prote No. 17.751 BB, Line No. 501-5MHz

Output Voltage from Generator

Operator - G.S. Hale, 20 September 1967

Pin NO. (Numbered from osc end)	Freq. 3 MHz		Freq. 7.2 MHz	
	Open	Short	Short	50 $\Omega$
1	.418	.357	.214	.276
2	.375	.391	.300	.273
3	.335	.433	.355	.268
4	.298	.470	.409	.264
5	.243	.500	.421	.252
6	.184	.528	.423	.258
7	.122	.549	.390	.253
8	.067	.560	.339	.252
9	.022	.567	.270	.252
10	.062	.565	.172	.251
11	.117	.554	.066	.251
12	.175	.540	.057	.252
13	.233	.518	.161	.252
14	.284	.490	.263	.252
15	.328	.458	.339	.252
16	.365	.417	.392	.253
17	.405	.372	.436	.253
18	.445	.332	.451	.253
19	.479	.296	.441	.256
20	.508	.243	.400	.257
21	.532	.184	.338	.257
22	.551	.120	.261	.257
23	.563	.062	.146	.257
24	.568	.000	.036	.258

Transmission Line Bridge Measurements

Assigned to Probe No. 17.751, Black Brant. Line No. 501-5MHz

Operator - G.S. Hale, 20 September 1967

Calibration Check Freq.	3 MHz		7 MHz	
End Measured	GSC End	Ant End	OSC End	Ant End
$Z_o C$	$6.8 + j54$	$6.9 + j55$	$20 + j92$	$19.5 + j90$
$Z_s C$	$3.8 - j42$	$3.9 - j43$	$5 - j27$	$5 - j28$
$Z_o = \sqrt{Z_{oc} Z_{sc}}$	47.7	48.7	51.0	51.0

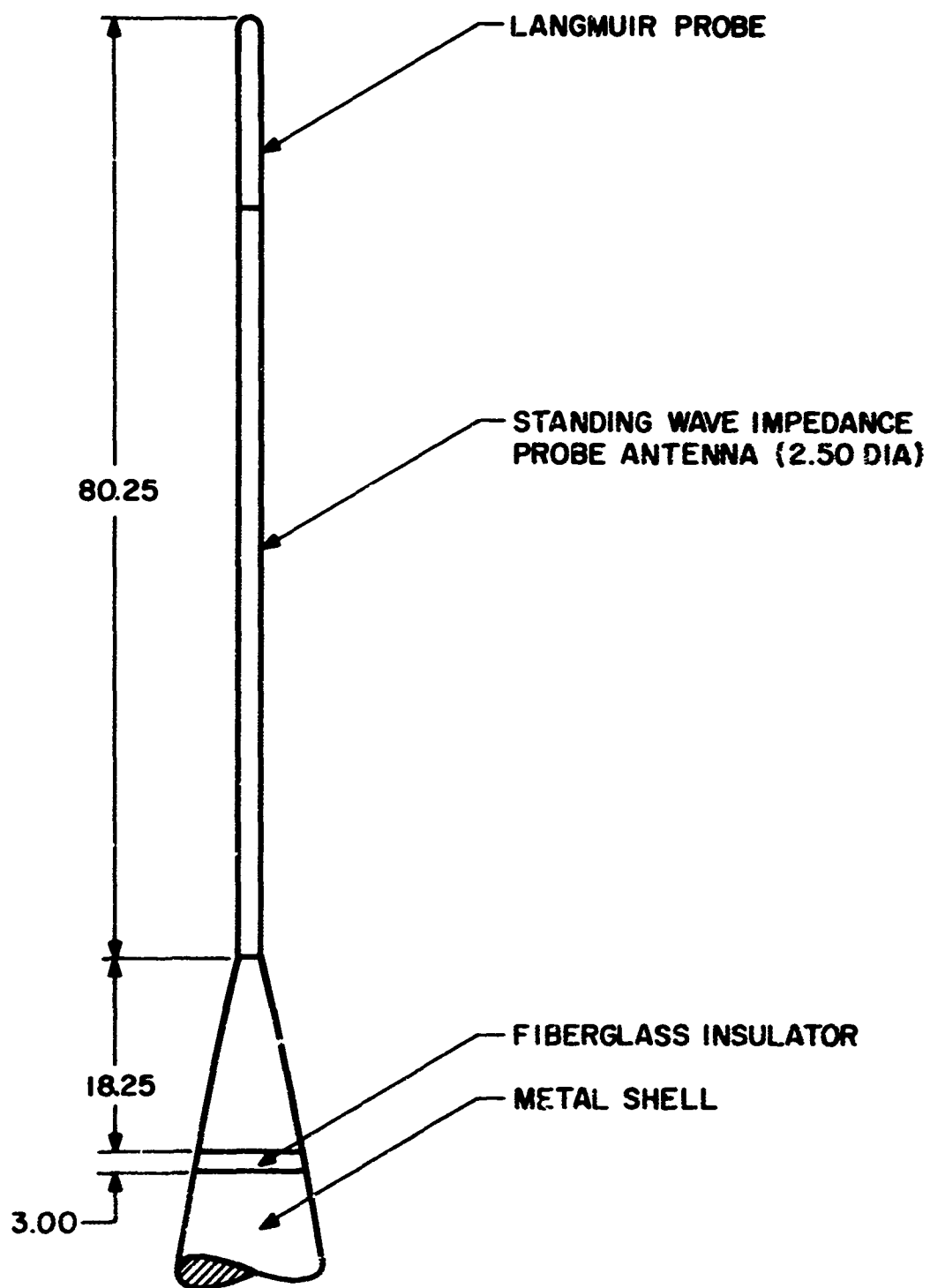


Fig. A-1. Physical dimensions (in inches) and orientation of the standing wave impedance probe antenna assembly on Black Brants 17.750 and 17.751.

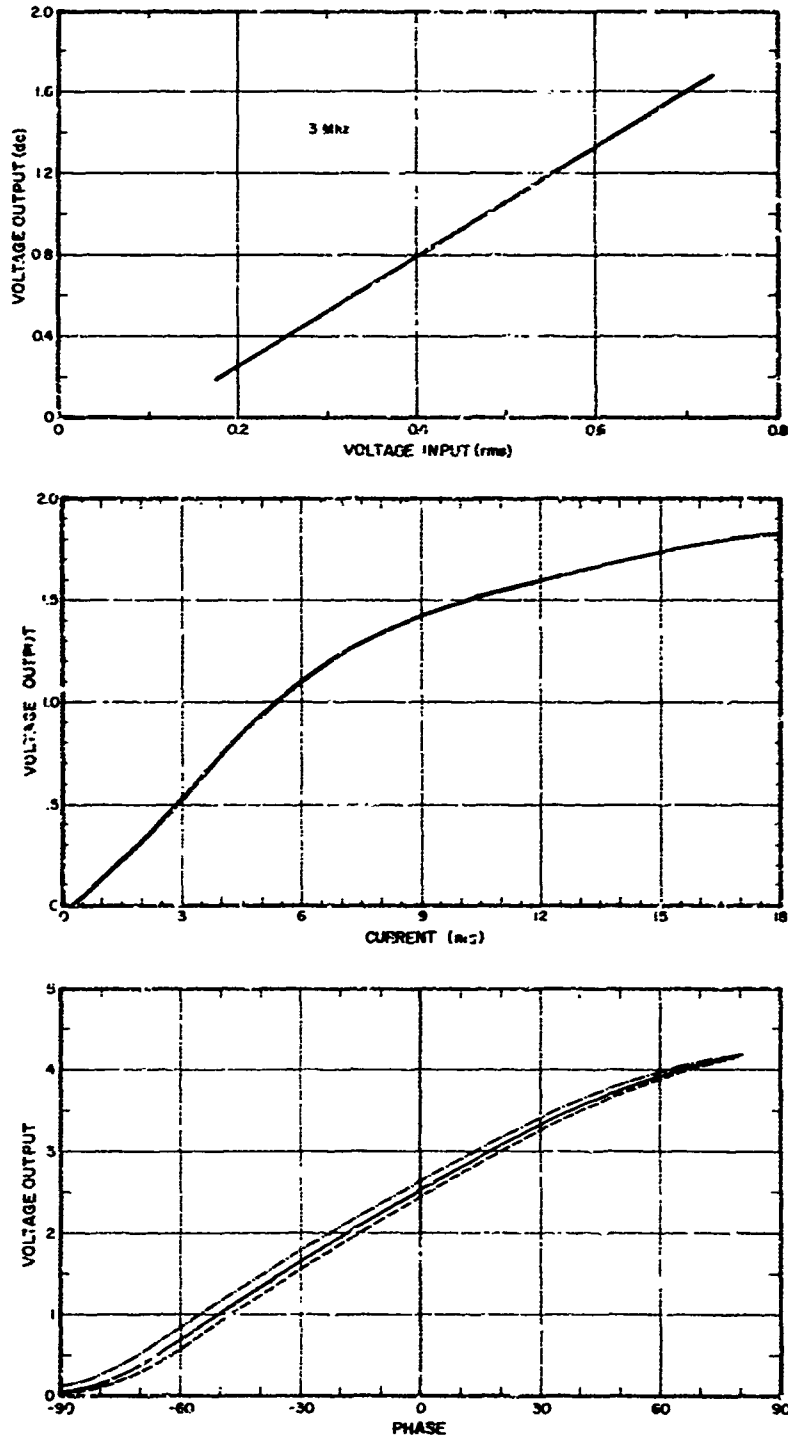


Fig. A-2. Voltage, current, and phase calibration curves at 3 MHz for the Z8 probe on 17.751.

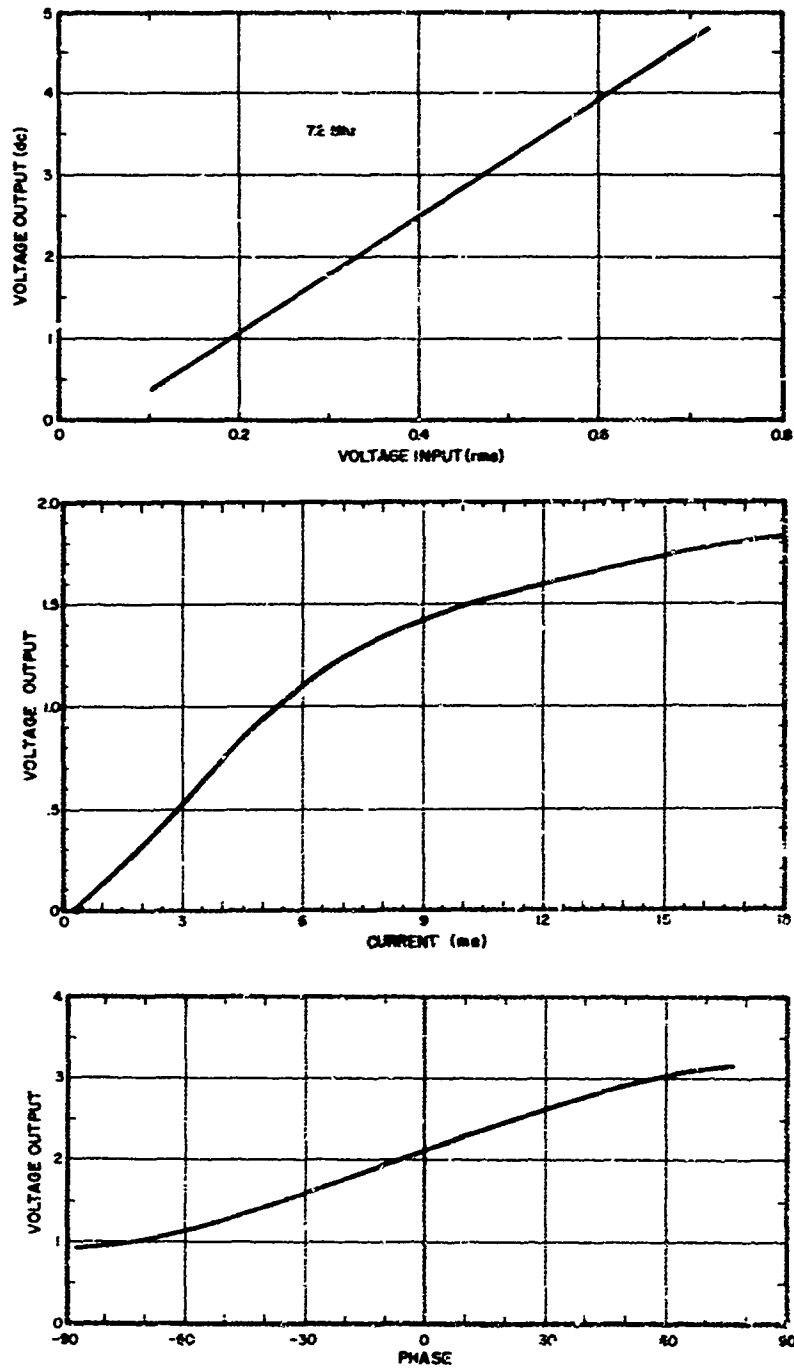


Fig. A-5. Voltage, current, and phase calibration curves at 7.2 MHz for the Z8 probe on 17.751.

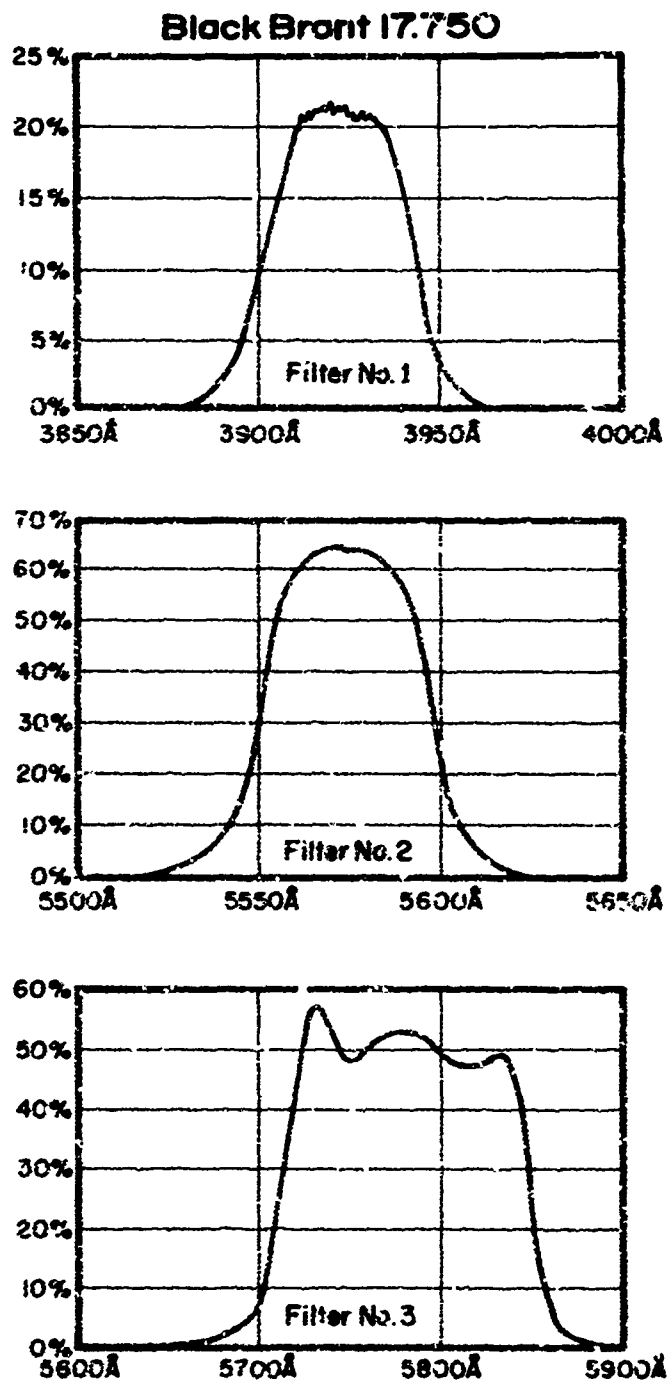


Fig. B-1 (a). Transmission curves for filters 1, 2, and 3 of the 17.750 filter wheel photometer (Model WT-1-B, SN-22-FW-1).

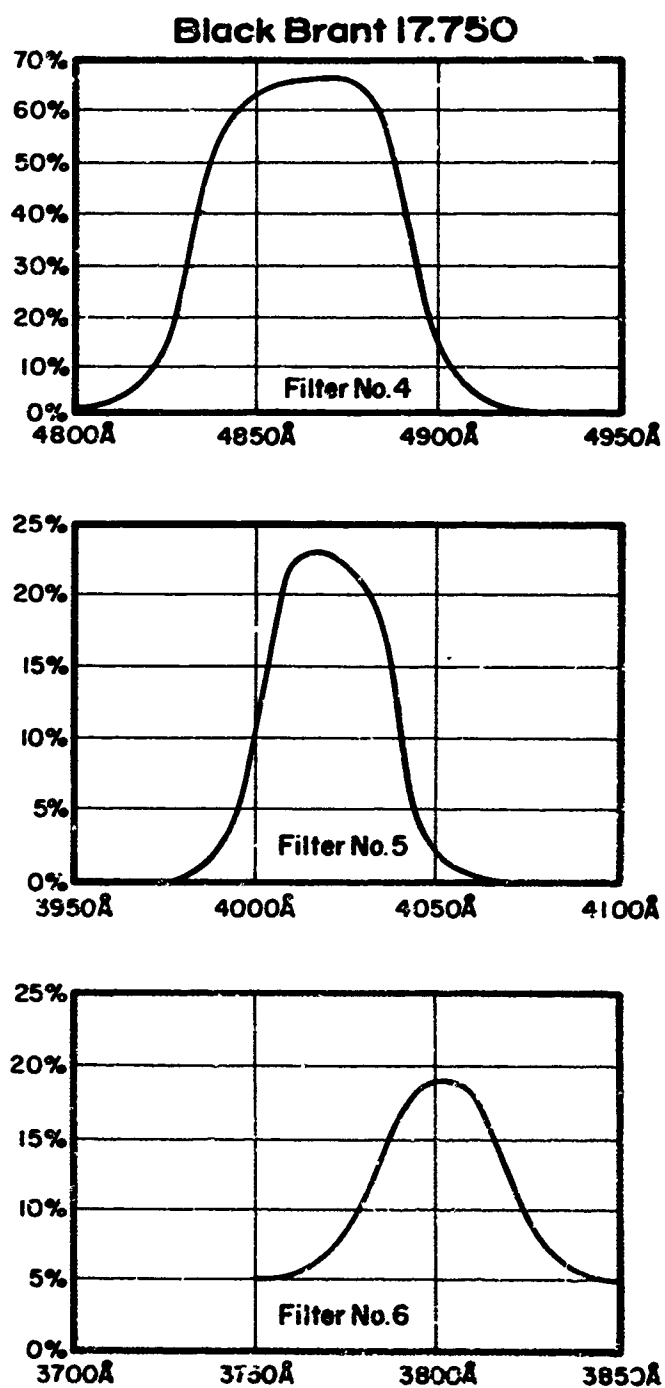


Fig. B-1 (b). Transmission curves for filters 4, 5, and 6 of the 17.750 filter wheel photometer (Model WT-1-B, SN-22-FW-1).

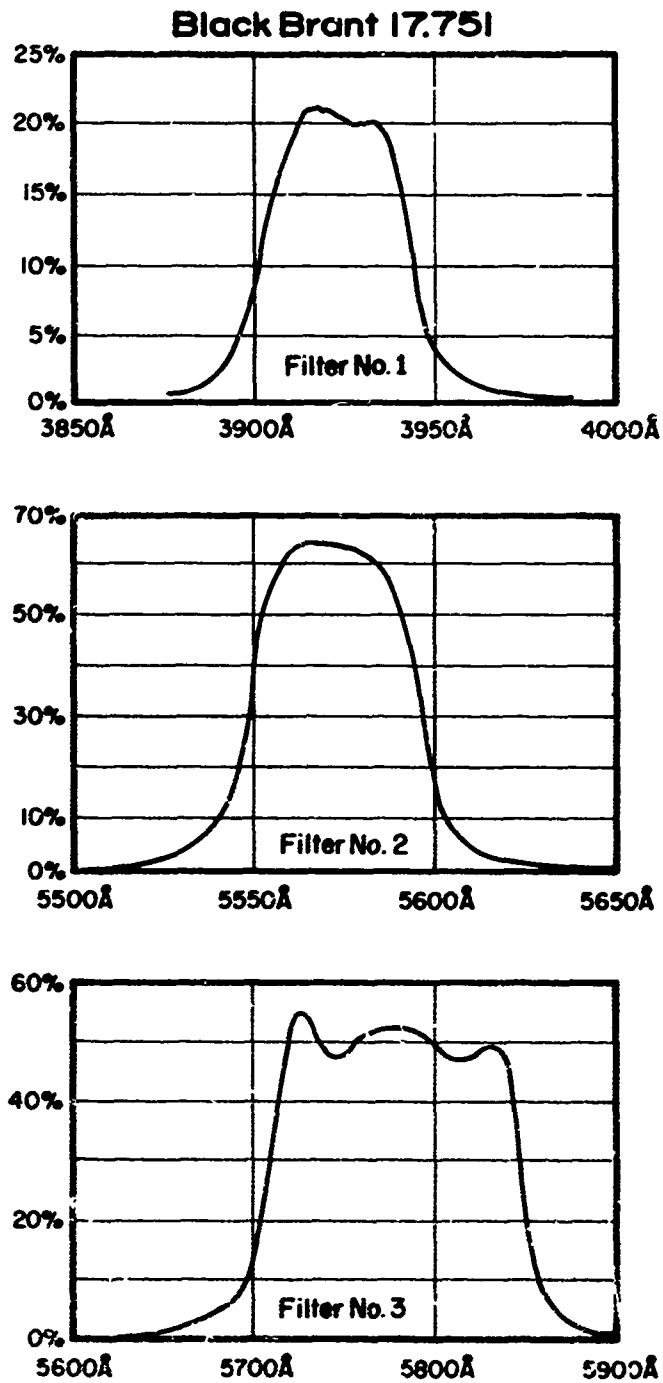


Fig. B-2 (a). Transmission curves for filters 1, 2, and 3 of the 17.751 filter wheel photometer (Model W1-1-B, SN-23).

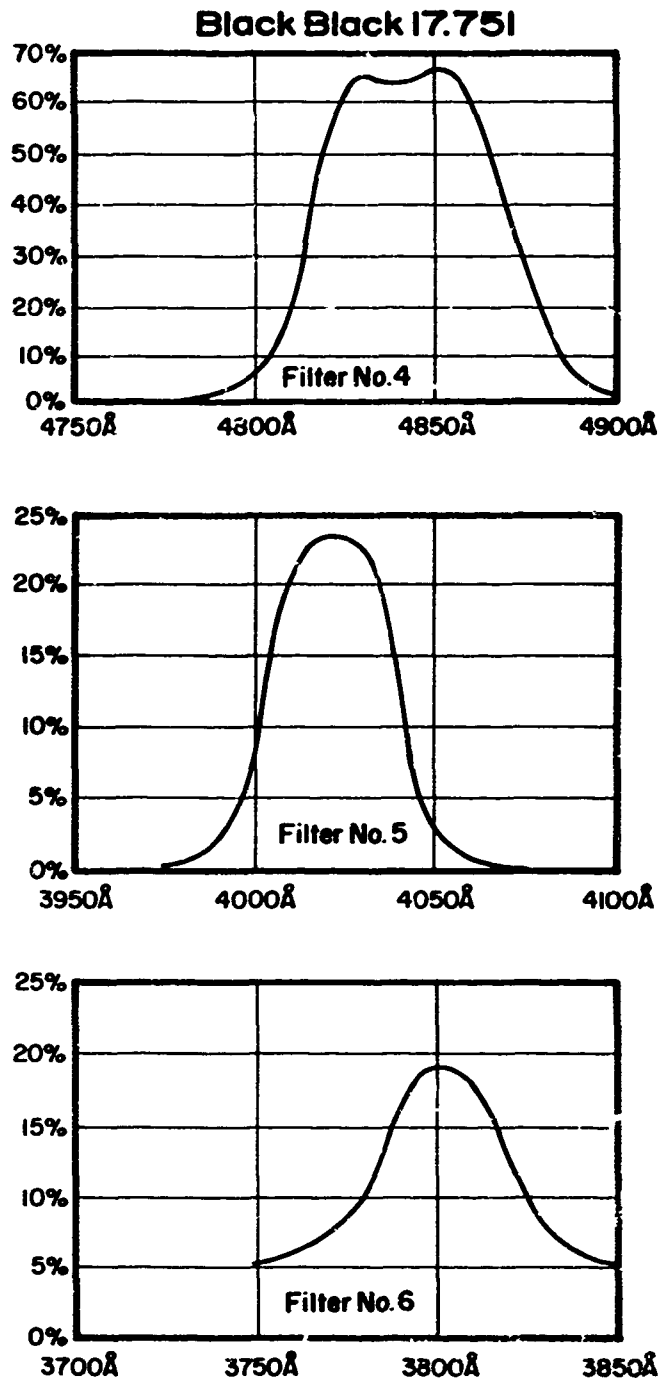


Fig. B-2 (b). Transmission curves for filters 4, 5, and 6 of the 17.751 filter wheel photometer (Model WT-1-B, SN-23).

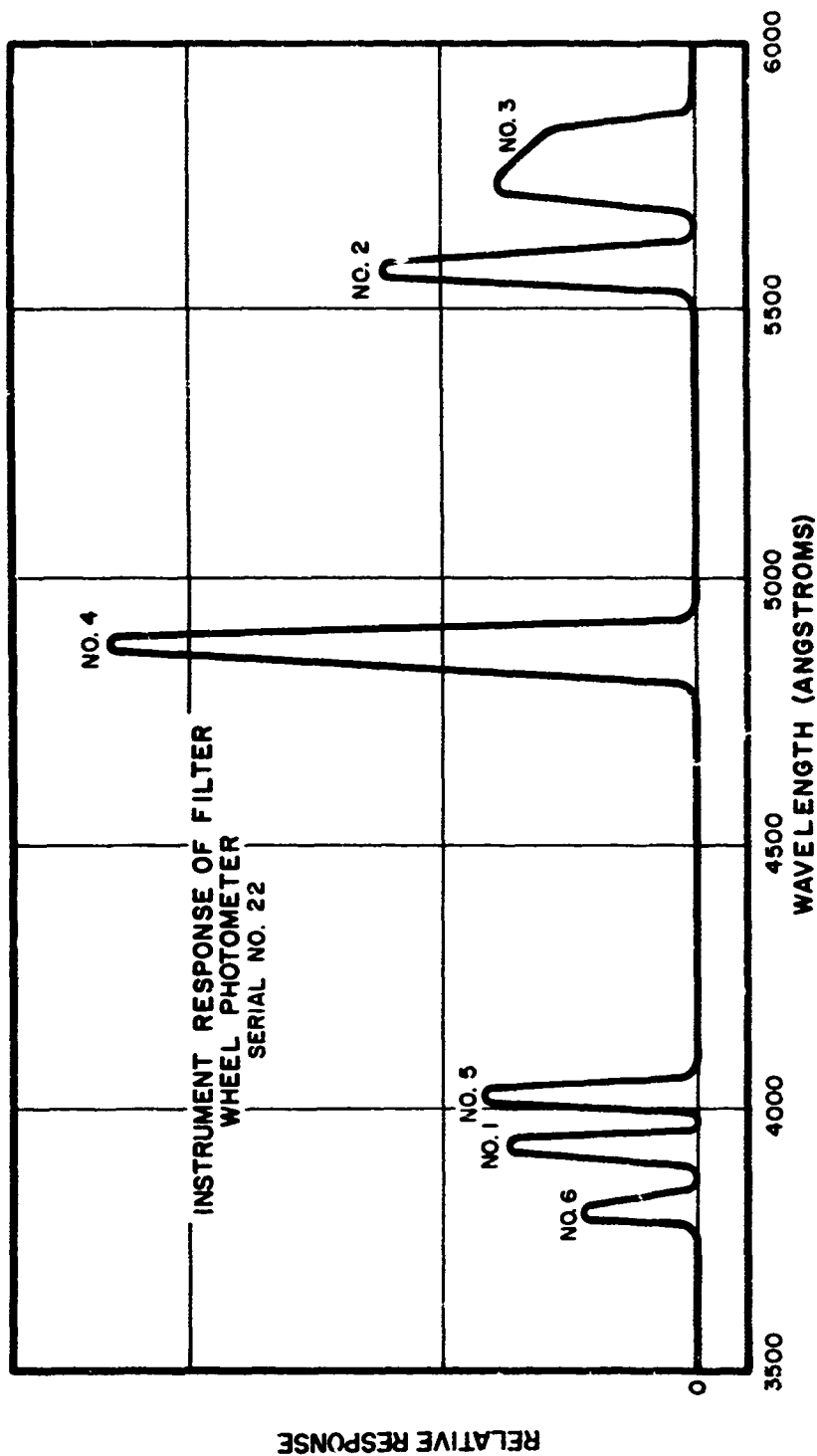


Fig. B-3, Composite spectral response of the filters on the 17.750 filter wheel photometer (Model WT-1-B, SN-22-FW-1).

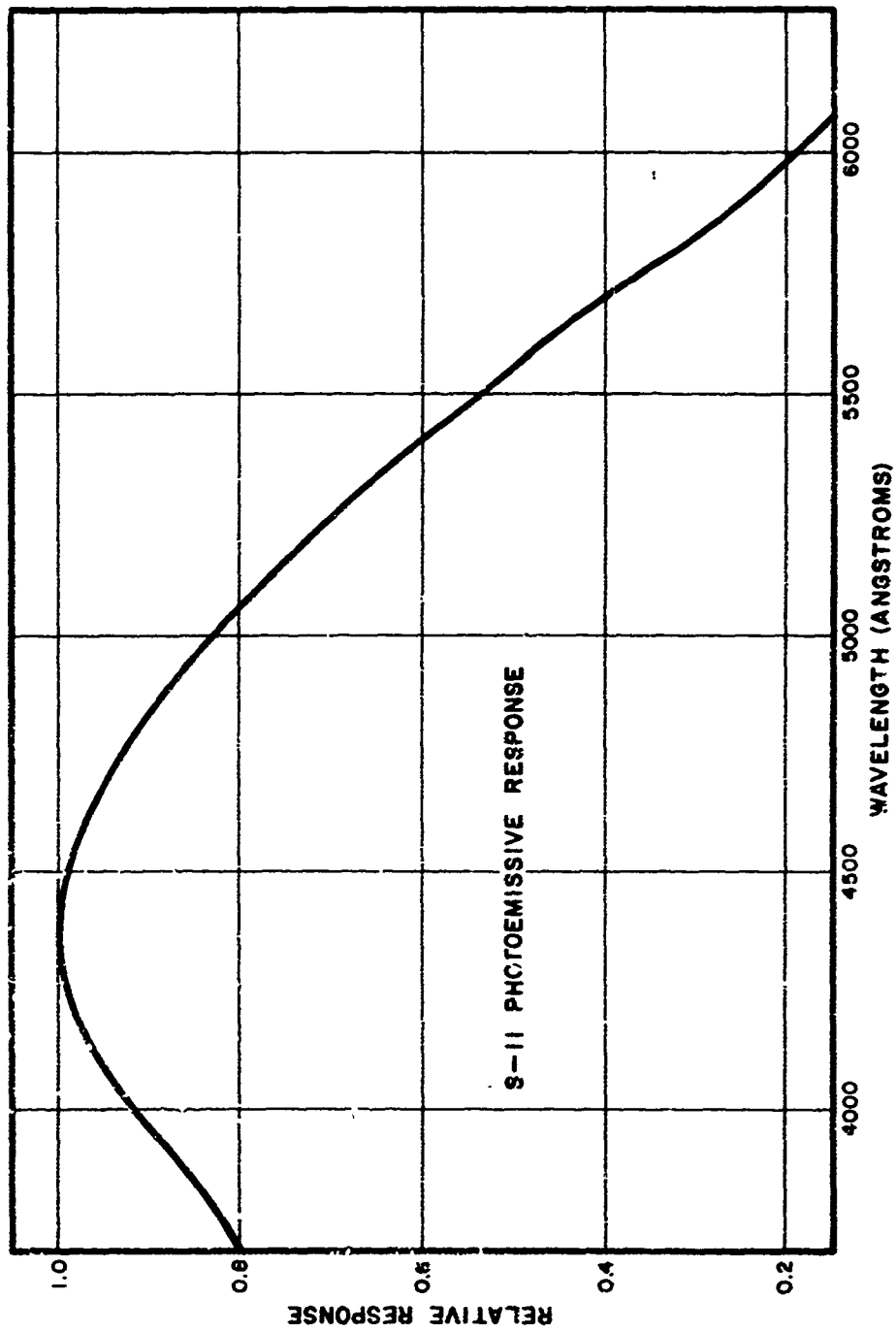


Fig. 3-4. Photoemissive response for S11 photomultiplier cathodes.

#### REFERENCES

- Burt, D.A., Rocket instrumentation for auroral measurements - Black Brant 17.604, *Scientific Report No. 7*, AFCRL 67-0295, Contract No. AF 19(628)-4995, University of Utah, Salt Lake City, 1967.
- Burt, D.A., and K.G. Seljaas, Rocket instrumentation for auroral measurements - Niros AD 7.618D and AD 7.619D, *Scientific Report No. 5*, AFCRL 66-738, Contract No. AF 19(628)-4995, University of Utah, Salt Lake City, 1966.
- Hinteregger, H., and L.A. Hall, Solar XUV radiation and neutral particle distribution in July 1963 thermosphere, *Space Research V*, edited by D.G. King-Hele *et al.*, 1175-1190, North Holland Publishing Co., Amsterdam, 1965.
- Howlett, L.C., Rocket-borne auroral x-ray instrumentation, *Scientific Report No. 2*, AFCRL 66-162, Contract No. AF 19(628)-4995, University of Utah, Salt Lake City, 1966.
- Seljaas, K.G., Langmuir probes for determining ionospheric particle densities and temperatures, *Scientific Report No. 1*, AFCRL 68-0306, Contract No. F19628-67-C-0275, University of Utah, Salt Lake City, 1968.
- Seljaas, K.G., and D.A. Burt, Rocket instrumentation for solar eclipse measurements - 12 November 1966, *Scientific Report No. 4*, AFCRL 67-0336, Contract No. AF 19(628)-5044, University of Utah, Salt Lake City, 1967.
- Ulwick, J.C., W. Pfister, O.C. Haycock, and K.D. Baker, Standing wave impedance probe, *COSPAR Technique Manual Series*, p. 66-89, edited by K. Maeda, 1967.

Unclassified  
Security Classification

DOCUMENT CONTROL DATA - R & D		
<i>(Security classification of title, body of abstract and indexing annotation must be entered when the overall report is classified)</i>		
1. ORIGINATING ACTIVITY (Corporate author) Upper Air Research Laboratory University of Utah Salt Lake City, Utah 84112		2a. REPORT SECURITY CLASSIFICATION Unclassified
		2b. GROUP
3. REPORT TITLE ROCKET INSTRUMENTATION FOR PCA MEASUREMENTS- BLACK BRANT 17.750 AND 17.751		
4. DESCRIPTIVE NOTES (Type of report and inclusive dates) Scientific. Interim.		
5. AUTHOR(S) (First name, middle initial, last name) David A. Burt		
6. REPORT DATE June 1969	7a. TOTAL NO. OF PAGES 79	7b. NO. OF REFS 7
8a. CONTRACT OR GRANT NO F19628-67-C-0275	DASA	9a. ORIGINATOR'S REPORT NUMBER(S) UU-69-2 Scientific Report No. 3
b. PROJECT NO. 5710		9b. OTHER REPORT NO(S) (Any other numbers that may be assigned this report) AFCR-69-0282
c. DoD Element: 61102H		
d. DoD Subelement: 68920G5088		
10. DISTRIBUTION STATEMENT 1-Distribution of this document is unlimited. It may be released to the Clearinghouse, Department of Commerce, for sale to the general public.		
11. SUPPLEMENTARY NOTES This research was supported by the Defense Atomic Support Agency	12. SPONSORING MILITARY ACTIVITY Air Force Cambridge Research Laboratories (CRP) L. G. Hanscom Field Bedford, Massachusetts 01730	
13. ABSTRACT This report discusses instruments contained in the payloads of Black Brants 17.750 and 17.751. These instruments were designed to measure characteristics of the D-region associated with polar cap absorption (PCA) events. The measurements included proton fluxes, x-ray emissions, total particle energy deposition, Lyman- $\alpha$ radiation, electron and ion densities and temperatures, and photometric emissions in the ionosphere. <span style="float: right;">alpha</span>		

DD FORM 1 NOV 65 1473

Unclassified  
Security Classification

Unclassified

Security Classification

14 KEY WORDS	LINK A		LINK B		LINK C	
	ROLE	WT	ROLE	WT	ROLE	WT
Rocket Instrumentation						
PCA Measurements						
Atmospheric Measurement Techniques						
D-Region Measurements						

Unclassified

Security Classification